Energetics of Zn^{2+} Binding to a Series of Biologically Relevant Ligands: A Molecular Mechanics Investigation Grounded on *Ab Initio* Self-Consistent Field Supermolecular Computations

NOHAD GRESH

Center for Advanced Research in Biotechnology, 9600 Gudelsky Drive, Rockville, Maryland 20850

Received 7 June 1994; accepted 1 November 1994

ABSTRACT

Detailed investigations are performed of the binding energetics of Zn^{2+} to a series of neutral and anionic ligands making up the sidechains of amino acid residues of proteins, as well as ligands which can be involved in Zn^{2+} binding during enzymatic activation: imidazole, formamide, methanethiol, methanethiolate, methoxy, and hydroxy. The computations are performed using the SIBFA molecular mechanics procedure (SMM), which expresses the interaction energy under the form of four separate contributions related to the corresponding *ab initio* supermolecular ones: electrostatic, short-range repulsion, polarization, and charge transfer. Recent refinements to this procedure are first exposed. To test the reliability of this procedure in large-scale simulations of inhibitor binding to metalloenzyme cavities, we undertake systematic comparisons of the SMM results with those of recent large basis set *ab initio* self-consistent field (SCF) supermolecule computations, in which a decomposition of the total ΔE into its four corresponding components is done (N. Gresh, W. Stevens, and M. Krauss, *J. Comp. Chem.*, **16**, 843, 1995). For each complex, the evolution of each individual SMM energy component as a function of radial and in- and out-of-plane angular variations of the Zn^{2+} position reproduces with good accuracy the behavior of the corresponding SCF term. Computations performed subsequently on di- and oligoligated complexes of Zn^{2+} show that the SIBFA molecular mechanics (SMM) functionals, E_{pol} and E_{ct}, closely account for the nonadditive behaviors of the corresponding second-

Present address: Laboratoire de Pharmacochimie Moléculaire, URA D1500 CNRS, U266 INSERM, Faculté de Pharmacie 4, Avenue de l'Observatoire, 75006, Paris, France.

Journal of Computational Chemistry, Vol. 16, No. 7, 856–882 (1995)

CCC 0192-8651 / 95 / 070856-27

order energy contributions determined from the *ab initio* SCF calculations on these complexes and their nonlinear dependence on the number of ligands. Thus, the total intermolecular interaction energies computed with this procedure reproduce, with good accuracy, the corresponding SCF ones without the need for additional, extraneous terms in the intermolecular potential of polyligated complexes of divalent cations.

Introduction

Zn^{2+} is a crucial cofactor within the active site of metalloenzymes such as thermolysin,[1] carboxypeptidase A,[2] carbonic anhydrase,[3] enkephalinase,[4] and the angiotensinogen-converting enzyme[5] (reviewed in refs. 6 and 7). It is mandatory for the structural stability of nonenzymatic proteins such as the so-called zinc-finger proteins.[8] A wealth of SCF *ab initio*[9-13] as well as semiempirical[14,15] supermolecule computations were devoted to a series of mono- and polyligated complexes of Zn^{2+}, in view of progressively reconstituting the enzymatic cavity and simulating the transition state. At the other extreme of the spectrum, extensive molecular mechanics and dynamics simulations were undertaken which dealt with complexes of a series of inhibitors with the entire protein, but resorting to highly simplified energy functionals (see, e.g., ref. 16 and refs. therein).

A rigorous understanding of the energetic involved in the binding of Zn^{2+} to its individual ligands, as enabled by accurate quantum-chemical computations, is warranted. This alone should provide the basis for reliable molecular mechanics functionals to be used in larger scale simulations of the Zn^{2+}-enzyme-inhibitor complexes, the size of which precludes the use of quantum chemistry. For that purpose, we have performed earlier[17,18] high-quality basis set *ab initio* SCF computations on the complexes of Zn^{2+} with the following series of neutral and ionic ligands: water, which is also the end sidechain of serine and threonine; formaldehyde, as a model for the carbonyl bond; formamide, which is the end sidechain of asparagine and glutamine as well as the building block of the protein backbone; imidazole, which is the end sidechain of histidine; methanethiol, which is the end sidechain of cysteine; formate, which is the end sidechain of aspartate and glutamate; methoxy, encountered as the alkoxy group in Zn^{2+}-mediated transition states of enzymatic catalysis[2]; OH^-, resulting from Zn^{2+}-assisted water deprotonation[9,19]; and methanethiolate, resulting from deprotonation of cysteine, occurring in the active site of cysteine protease enzymes,[20] and encountered in the structure of the mercaptan class of metalloenzyme inhibitors.[21] For each complex, we have undertaken a breakdown of the supermolecular interaction energy into its four components: Coulomb and exchange at first order; and polarization and charge transfer at the second order. This was done with the restricted variational space (RVS) analysis procedure due to Stevens and Fink.[22] In this article, we will first present novel refinements of the SIBFA[23-25] molecular mechanics procedure (denoted as SMM). These bear principally on the two second-order terms, the weight of which is particularly amplified in divalent cation–ligand complexes. For each Zn^{2+}–ligand complex, we will then monitor the evolutions of each SMM energy contribution as a function of radial as well as in- and out-of-plane variations of the position of Zn^{2+} and compare them to those of the corresponding *ab initio* SCF supermolecular energy components.

We follow the same approach as in ref. 17. We perform first variations of the distance, R, of Zn^{2+} located in the ligand plane, with respect to its electron-donating heteroatom, at a well-defined angle: thus, upon binding to water, imidazole, and methanethiol, the cation lies along the external bisector of the angle centered on the oxygen, the pyridinelike nitrogen, and sulfur, respectively; upon binding to carbonyl, carboxylate, methoxy, hydroxy, and thiolate, it lies along the direction of the bond bearing the heteroatom. This will enable us to calibrate, in the SMM procedure, a limited set of parameters on each ligand: These are the effective radii W, V, and U of the heteroatom, which intervene in the expressions of the short-range repulsion, the polarization, and the charge transfer, respectively; and the E and F parameters, which intervene as the preexponential factor and as the exponent, respectively, in the expression of the Gaussian screening factor of the electrostatic field. The validity of the calibration will be assessed by performing in the next step: first, in-plane variations of the θ angle, which denotes the

angles H—O—Zn, C—N—Zn, C—O—Zn, and C—S—Zn, according to the ligand investigated; second, out-of-plane variations of Zn^{2+}, as quantified by variations of a dihedral ϕ angle. The calibration of the increments of effective radii U and W of the heteroatoms' π lone pairs with respect to the σ ones (generally in between 0.0 and 0.3) is done for the value of $\phi = 90°$, to improve the fit of E_{rep}(SMM) and E_{ct}(SMM) to their SCF RVS counterparts for this angular value.

Such detailed explorations, bearing on nine Zn^{2+}–ligand complexes, will constitute demanding tests of our molecular mechanics energy procedure and the reliability of each of its individual components. There is to our knowledge no precedent for any other similar investigation.

The last step of this investigation is devoted to di- and oligoligated complexes of Zn^{2+}. We will test the extent to which the separate nonadditive behaviors of E_{pol} and E_{ct} of the *ab initio* supermolecular computations, reported earlier,[17] can be accounted for by the corresponding SMM terms. It will be shown that a close reproduction is indeed possible without resorting to extraneous many-body formulas. This important finding should ensure the transferability of the SMM expressions to a wide variety of metal–ligand complexes.

Finally, despite the considerable interest aroused by Zn^{2+} interactions, it is only due to our knowledge of the pioneering investigations of refs. 9 and 10 that, prior to the present endeavors,[17,18] an explicit breakdown of the SCF supermolecule intermolecular interaction energy of Zn^{2+} to nonwater ligands was reported, and for other than mere variations of the cation–ligand distance.

Procedure

AB INITIO SUPERMOLECULE COMPUTATIONS

The energy decomposition reported in refs. 17 and 18 used the RVS procedure due to Stevens and Fink.[22] Because of its fully variational nature, there is no E_{mix} term as in the Morokuma procedure,[26] the large amplitude of which in divalent cation–ligand complexes (see ref. 27 and C. Giessner-Prettre, unpublished results) can prevent the deconvolution of E_2 into its separate polarization and charge transfer terms. In addition to refs. 17 and 18, the RVS procedure was recently applied in a joint SCF/density functional theory/molecular mechanics investigation devoted to a series of neutral and anionic H-bonded complexes.[28] Its principles were exposed in the original article[22] and recalled in refs. 17 and 18. The C, N, O, and S core, and the first two occupied shells of Zn^{2+}, are represented by the atomic compact effective potentials derived by Stevens et al.[29] The H basis set consists of four Gaussians, contracted (3, 1). The valence basis sets of the heavy atoms also consist of four Gaussians, contracted (3, 1). With respect to the basis sets originally derived in ref. 29, the heavy atoms are supplemented with a set of two diffuse, uncontracted 3*d* orbitals. Further details of the basis sets used and of the decomposition strategy are given in refs. 17 and 18.

In the *ab initio* computations of ref. 17, correlation effects were not included. MP2 computations were performed in ref. 18, restricted, however, to single-point computations at the HF/energy-optimized position. A molecular mechanics fitting of the MP2 correction by an expansion into $1/R^{**}6$, $1/R^{**}8$, and $1/R^{**}10$ terms,[30] similar to our aforementioned study of H-bonded complexes,[28] and a generalization to the cations Mg^{2+}, Ca^{2+}, and Cd^{2+} will be undertaken in a forthcoming study. The basis set superposition errors (BSSE) were shown in refs. 17 and 18 to be small on account of the large basis sets used and will therefore not be taken into account in the SMM versus SCF comparisons.

MOLECULAR MECHANICS COMPUTATIONS

The SIBFA (Sum of Interactions between Fragments *Ab Initio* Computed) procedure[23–25] differs from standard molecular mechanics procedures by the following salient features:

—The electrostatic energy is computed by means of a multipolar, multicentered expansion derived from the SCF molecular wave function of the individual monomers, following a procedure due to Vigné-Maeder and Claverie.[31]

—The short-range repulsion is computed as a sum of bond–bond, bond–lone pair, and lone pair–lone pair interactions, rather than a sum of atom–atom pairwise interactions, to account for its anisotropic behavior.

—Explicit expressions are included for the individual second-order polarization and charge transfer components.

The functional forms used in this work are similar

to those used previously in the development of the SIBFA procedure. However, they have been modified and recalibrated in light of the results now available from the RVS procedure, which provided separate values for E_{pol} and E_{ct}, and from the recourse to significantly improved basis sets, which uncovered more complex behaviors of the first-order *ab initio* terms, Coulomb (E_c) and short-range repulsion (E_e), than the ones obtained previously with small basis sets. These functional forms are as discussed next.

Electrostatic Term, E_{MTP}

This term is computed using the distributed multipoles from the large basis set computations on the isolated fragments, rather than those from the SIBFA standard library of fragments, which used small basis set computations. The importance of this factor will be discussed later.

Short-Range Repulsion Term, E_{rep}

To confer an anisotropic behavior to the term representing the exchange repulsion, several distinct formulations have been proposed (reviewed in ref. 32). These include explicit consideration of the lone pair directionality,[23-25] reduction of the interatomic distance intervening in the exponential factor by an orientation-dependent term,[33-36] and explicit numerical fitting to a very large number of *ab initio* supermolecule computations of E_e by means of a series of cosine terms in the preexponential term.[37] The formulation used here is related to the preceding SIBFA approach.[23-25] The E_{rep} term is related to the overlap of the fragment densities and is expressed as a sum of pairwise interactions between the localized bonds and lone pairs of the individual ligands. Such localized representations introduce a natural anisotropy into the repulsive interactions. In the SIBFA algorithm, the repulsive interaction, E_{rep}, is proportional to the square of the overlap (S^2) between the interacting electron densities.[38] It has been suggested[39,40] that proportionality to S^2/R, where R is the distance between fragments, may be more appropriate, and this has been found to be true in the present study.

In the general case of molecule A with bonds PQ and lone pairs L_α interacting with molecule B with bonds RS and lone pairs L_β, the general expression for E_{rep} is

$$E_{rep} = C_1\Big(\sum_{PQ}\sum_{RS} \mathrm{rep}(PQ, RS) + \sum_{PQ}\sum_{L_\beta} \mathrm{rep}(PQ, L_\beta) + \sum_{L_\alpha}\sum_{RS} \mathrm{rep}(L_\alpha RS) + \sum_{L_\alpha}\sum_{L_\beta} \mathrm{rep}(L_\alpha L_\beta)\Big) \quad (1)$$

When one of the interacting species is a spherical atom or ion, M, the localized lone pairs may be replaced by a spherical density. In that case, the expression reduces to

$$E_{rep} = C_1\Big(\sum_{PQ} \mathrm{rep}(PQ, M) + \sum_{L_\alpha} \mathrm{rep}(L_\alpha, M)\Big) \quad (2)$$

Treatment of the Bond/Cation Repulsion. In the original SIBFA formulation, the molecular orbital (MO) localized in bond PQ was implicitly approximated by a sum of two spherical densities located on atoms P and Q. Hybridization was taken into account only for lone pair orbitals. The current formulation introduces hybridization at the level of bond PQ as well. The bond is represented by idealized atomic hybrid orbital constructs, which are taken as standard admixtures of s and p Slater-type exponential functions with fixed exponents for each type of atom. Given the hybridization coefficients and the geometry of the hybrid orbital/metal cation interaction, the overlap density contributions are easy to calculate. For example, in keeping with refs. 24 and 25, the overlap density S_{PM} between the $2s$ component of P and the pure ns density on metal cation M, $\langle 2S_P \mid nS_M \rangle$ is given by

$$S_{PM} = M_{PM} \exp(-\alpha \rho_{PM}) \quad (3)$$

where

$$\rho_{PM} = r_{PM}/4\,\mathrm{sqrt}(W_P W_M) \quad (4)$$

and

$$M^2_{PM} = K_{PM}(1 - Q_P/N^P_{val}) \quad (5)$$

where r_{PM} denotes the interatomic distance between P and M, W_P and W_M are the effective radii of P and M, Q_P is the electronic population on P (the Mulliken net charge), N^P_{val} is the number of valence electrons of P (6 for O, 5 for N, etc.), and

K_{PM} is the product of two adjustable atomic parameters $K(Z_P)$ and $K(Z_M)$. In eq. (4), the effective atomic radii, W_P and W_M, modulate the magnitude of the reduced distance, r_{PM}, which appears in the exponential term in eq. (3). Equation (5) relates the amplitude of the preexponential factor, M_{PM}, to the electronic population of atom P (see ref. 39 for a more complete discussion). Thus, more electron-rich atoms will have larger preexponential factors in the overlap density expression. Such a modulation is not done in the case of closed-shell metal cations. With respect to the corresponding formulation in ref. 24, the M^2 factor is no longer divided by the sum of the lone pairs and chemical bonds originating from P. (Independent computations in which this division was maintained did not improve the behavior of E_{rep} when compared to E_e).

Equations for overlap between the p components of the ligand atomic hybrids and the metal orbitals are similar, except for an angular factor. For simplicity, the following relationship between the p and s contributions to the ligand–metal overlap is assumed:

$$\langle 2p_{\sigma P} \mid nS_M \rangle = m_{PM} \langle 2S_P \mid nS_M \rangle \qquad (6)$$

where $2p_\sigma$ denotes the p component along the line connecting the ligand and metal atoms. The proportionality factor, m_{PM}, is characteristic of the pair PM involved and is taken as constant over the range of distances investigated around equilibrium (see refs. 24 and 25 for details). The overlap, O(PQ, M), between the electronic distributions of bond PQ and metal M can be expressed as a function of the S_{PM} and S_{QM} terms weighted by the appropriate hybridization coefficients, the m_{PM} and m_{QM} factors, and the appropriate angular factors. The contribution of this overlap term to the exchange repulsion interaction is taken as

$$\text{rep(PQ, M)} = N_{occ}(\text{PQ}) O^2(\text{PQ, M})/D_{\text{PQ, M}} \qquad (7)$$

where $D_{\text{PQ, M}}$ is the distance between the midpoint of bond PQ and atom M. This assumes (as outlined earlier) a dependence of E_{rep} proportional to S^2/R, rather than to S^2.

Treatment of the Lone Pair / Cation Repulsion. Similar formulas as the foregoing and as in ref. 24 apply to the lone pair/cation repulsion, except that the repulsion term is taken as

$$\text{rep}(L_\alpha M) = N_\alpha O^2(L_\alpha, M)/D_{BM} \qquad (8)$$

where N_α denotes the occupation number of the lone pair orbital: 2.0 for *sp*-hybrid lone pairs, and 1.0 for each lobe of a pure π lone pair. D_{BM} is the distance between the atom bearing the lone pair orbital and the metal cation.

Polarization Energy Term, E_{pol}

The large, directional electric fields generated by the divalent cation make it necessary to have a good description of the anisotropy of the polarizabilities of the ligands[41] in the molecular mechanics treatment. To ensure this, a procedure developed by Garmer and Stevens[42] has been used, in which the polarizabilities are derived from finite-field SCF computations using localized orbitals. This procedure was incorporated by these authors in the Hondo[43] code (W. J. Stevens, and D. R. Garmer, Center for Advanced Research in Biotechnology, unpublished). The local polarizabilities are distributed on the centroids of the chemical bonds and the lone pairs of the molecule. The transferability of bond and lone pair polarizabilities defined in this way has been demonstrated to be good.[42] The use of anisotropic polarizabilities represents a modification of the SIBFA procedure, which formerly used isotropic atomic polarizabilities.

The calculation of the polarization energy for multiple interacting species proceeds as follows. If P is a polarizable point in ligand A, the ith Cartesian component of the dipole moment, $\mu_P^{ind}(i)$, induced by the jth component of the electric field, $E_P(j)$, at point P is given by

$$\mu_P^{ind}(i) = \alpha_P(i, j) E_P(j) \qquad (9)$$

where $\alpha_P(i, j)$ is an element of the polarizability tensor. The electric field at point P is given by

$$E_P(j) = \sum_{B \neq A} \sum_{Q \in B} E_{Q \to P}(j) \qquad (10)$$

where B denotes every molecule that interacts with A in an intermolecular complex, and Q denotes every point in B that gives rise to an electric field at P.

The polarization energy contribution from point P can be expressed as

$$E_{pol}(P) = -0.5 \sum_i E_P(i) \mu_P^{ind}(i) \qquad (11)$$

In the most general case, the electric field at P contains contributions from induced dipoles in

molecules B, and an iterative procedure must be used to achieve self-consistency of the induced moments. However, in the systems under study here, the divalent metal cation dominates the electric field seen by the ligand, and the polarizability of the cation (and hence self-consistency) is neglected.

The components of the electric field vector generated at point P in the ligand by the charge at the metal cation center, M, are calculated using standard formulas (see, e.g., refs. 44 and 45). It is necessary to reduce $E_{pol}(P)$, however, to account for the screening of the incoming polarizing charge by the electronic cloud of P. For simplicity, we introduce a Gaussian screening function $S(P,M)$, such that

$$E_{M\to P} = (1 - S(M,P))E^0_{M\to P} \quad (12)$$

$$S(M,P) = Q_M E \exp\left(-F\left(R^{**2}_{PM}\right)/(V_P + V_M)\right) \quad (13)$$

where R_{PM} is the distance between the metal cation and the polarizable point, and V_M and V_P are the effective radii of the metal and the polarizable electronic cloud. Analysis of the *ab initio* E_{pol} energy behavior for ligands with large polarizations revealed a penetration effect that was more strongly R-dependent than the simple Gaussian cutoff function. This effect was mimicked in the molecular mechanics procedure by increasing the effective radius of the polarizable distribution by an amount proportional to the induced dipole moment in the direction of the polarization. Thus, the effective radius is given by

$$V_P = V^0_P + G|\mu^{ind}_P| \quad (14)$$

Within the iterative procedure, only the monopolar contributions are used to compute $E_{M\to P}$, and the effect of the induced dipole on the cation, as mentioned earlier, is not taken into account. Upon considering the polyligated complexes of Zn^{2+} (*vide infra*), a more complete representation, including a complete multipolar field and the effect of the induced dipoles on other-than-metal centers, will be evaluated.

Whereas E, F, and G are parameters which can be adjusted for each ligand, V_P and V_M denote the effective radii of A and M (*vide infra*), and $|\mu^{ind}_P|$ denotes the norm of the dipole induced on A, which is proportional to the polarizing field computed at the preceding iteration. In this formulation, the effective radius, V_P, of the polarizable center P, involved in the screening of the field E_P, is increased in proportion to the field. Such an iterative derivation of S was found in some instances to improve by 2 kcal/mol the match of E_{pol} to the corresponding SCF value as compared to an alternative, noniterative procedure, in which the effective V_P radii were tentatively assigned empirical increments as input data to fit the SCF results.

In eq. (13), we have also resorted to the absolute value of the monopolar charge, Q_M, of M. Whereas removing it from the expression of $S(P,M)$ would not affect the quality of the results obtained for E_{pol} in the Zn^{2+} monoligand interactions (and would simply be compensated for by doubling the value of E), its presence was found to improve significantly the value of this contribution in other complexes, such as the water dimer, for which there are partial charges on the polarizing molecule dictated by the electronic distribution.

Charge Transfer Energy Term, E_{ct}

In the SIBFA method, the perturbative expression[46] used in refs. 24 and 47 for E_{ct} involving a cation as the electron acceptor is

$$E_{ct} = -2S_M \sum_{\alpha} N_{occ}(\alpha)\left((I_{\alpha M^\wedge})^{**2}/\Delta E_{\alpha M^\wedge}\right) \quad (15)$$

in which $M^\wedge$ defines the excited state of the cation and in which the summation runs over all lone pairs of the electron-donor molecule A, S_M is a constant which is characteristic of the cation, and $\Delta E_{\alpha M^\wedge}$ is a difference between the ionization potential of the lone pair L_α and the electron affinity of the electron acceptor $M^\wedge$.

The integral $I_{\alpha M^\wedge}$ has the form

$$I_{\alpha M^\wedge} = \exp(-\eta\rho_{AM^\wedge})N_{AM^\wedge} (C_s t_{AsM} + C_p m_{AM} t_{ApM} \cos\omega_M) \quad (16)$$

with

$$N_{AM^\wedge} = (D_M F_M) - V \quad (17)$$

In eq. (16), ω_M denotes the angle, centered at A, between the direction of the lone pair L_α and that of the segment linking A to M. η is an adjustable constant, and $\rho_{AM^\wedge}$ is a reduced radius expressed in terms of the interatomic distances $R_{AM^\wedge}$ and the effective radii U_A and U_M:

$$\rho_{AM^\wedge} = R_{AM}/(4\,\mathrm{sqrt}(U_A U_{M^\wedge}) \quad (18)$$

C_s, C_p, and m_{AM} have the same meaning as in the expression of E_{rep} (the overlap integrals now in-

volving the 4s orbitals of the cation). t_{AsM} and t_{ApM} are factors of proportionality which are used to partition the hybrid integrals $\langle 2S_A|V|nS_M\rangle$ and $\langle 2p_{\sigma A}|V|nS_M\rangle$ onto the distributions $(2S_A\ 2S_A)$, $(2p_{\sigma A}\ 2p_{\sigma A})$, and $(nS_M\ nS_M)$. They are expressed in terms of the overlap integrals $\langle 2S_A \mid nS_M\rangle$, $\langle 2p_{\sigma A} \mid nS_M\rangle$, and corresponding overlap dipole moment integrals, as computed with standard Slater atomic orbitals (AOs) (see refs. 24, 25, and 47 for derivation of these expressions). V is the electrostatic potential exerted by the cation on the lone pair barycenter, D_M is a calibration constant characteristic of the cation, and F_M is the self-potential of M, which can be expressed as

$$\langle nS_M \mid V_M \mid nS_M\rangle_{\rho\to 0} = F_M = \zeta_M Z_M/(nS_M + 1) \quad (20)$$

upon extrapolation at $\rho \to 0$ of the value of the Coulomb integral of the electrostatic potential Z_M/R exerted by M and computed with Slater orbitals over its own distribution nS_M (see refs. 24, 25, and 47 for additional details), ζ_M denoting the Slater exponent of the first vacant orbital of M.[48]

Three important modifications were added to this formulation. The large charge transfer effects associated with the divalent cation which were uncovered by the RVS analysis prompted us to account for self-consistent effects in both the mono- and polyligated complexes.

1. The first related to the numerator term $N_{AM^\wedge}$. Let us denote by C all those atom centers belonging to any molecule other than A and distinct from M so that, for example, $V_{C\to M}$ and $V_{C\to A}$ are the electrostatic potentials generated by C on M and A, respectively. Then

$$N_{AM^\wedge} = (D_M F_M) + \sum_C V_{C\to M} - \left(V_{M\to A} + \sum_C V_{C\to A}\right) \quad (21)$$

Note that the V terms encompass both the static potentials and the potentials due to the induced dipoles on C and A via their polarizabilities, thus introducing an implicit coupling between charge transfer and electron-donor polarization.

2. The second modification relates to the denominator $\Delta E_{\alpha M^\wedge}$. The electron affinity, $A_{M^\wedge}$, of Zn^{2+}, is 18 eV,[49] whereas the lone pair ionization potentials, for the water oxygen, carbonyl oxygen, and anionic oxygen, amount to 12.8 eV,[50] 10.9 eV,[51] and 4.4 eV, the latter value resulting from our own SCF computations in formate. The difference $I_{L_\alpha} - A_{M^\wedge}$ is then systematically negative, whence a positive value of E_{ct}, which corresponds to a different, open-shell complex (i.e., $M^+ - L^+$) from the one investigated with the restricted Hartree-Fock formalism, which retains a dipositive cation. However, the significant perturbation due to the cationic charge results in a lowering of the electron-donor HOMO ionization potential, which, in representative Zn^{2+}–ligand complexes, was found to be approximately proportional to the electrostatic potential exerted on it. We are thus led to take into account such an energy-lowering effect in the denominator. We similarly take into account a concomitant reduction of the cation electron affinity due to the electrostatic potential of the surrounding ligand(s). Then

$$\Delta E_{\alpha M^\wedge} = \left(I_{L_\alpha} + V_{M\to A} + \sum_C V_{C\to A}\right) - \left(A_M + V_{A\to M} + \sum_C V_{C\to M}\right) \quad (22)$$

Note again that the V terms encompass the potentials generated by the induced dipoles as well.

3. The third modification relates to the exponential term. As we have seen for the polarizability, the effective radius, U_A, of the electron donor is increased in an anisotropic fashion, in the direction of the electric field it senses and proportional to the field's magnitude. An additional modulation was also tentatively introduced through the magnitude of the field undergone by the electron acceptor itself, E_M, and was introduced to fit the results obtained in the dihydrated, inner-shell complexes of Zn^{2+}. The expression adopted is

$$U_A = U_A^\circ + I((|E_A| - J|E_M|)^{**2})|\cos\omega_M| \quad (23)$$

where I and J are adjustable constants and U_A° is the effective radius of the donor in the absence of external field.

Our SMM formulation of repulsion and charge transfer, which are both predominantly overlap dependent, resorts to a formalism in terms of bond

and lone pair orbitals. However, the two representations differ upon dealing with π-type bonds. The polarizabilities are located on the centroids of banana bonds, whereas for E_{ct} and E_{rep} the lone pairs are located at the heteroatom extremity of the bond, perpendicular to the plane of the conjugated molecule, and with an occupation number of one.

CALIBRATION OF THE SMM PROCEDURE

Each of the separate SMM contributions to the binding energy was calibrated by adjusting the free parameters to fit the SCF supermolecule counterpart in the Zn^{2+}–water complex. Zn^{2+} was constrained to lie in the water plane, along its external bisector. Seven Zn—O distances at 0.1 Å spacing were selected from 1.7 Å to 2.3 Å. With the exception of the following, the parameters thus derived were found to be transferable to all mono- and polyligated Zn^{2+} complexes subsequently investigated:

—The E and F parameters, occurring in the screening of the electrostatic field [see eq. (14)]. Individual values for the representative ligands of this study are given in the Appendix. With the exception of imidazole, the E values are in the range 0.65–0.78, and the F values are in the range 1.40–1.65.

—The J parameter in the exponent of E_{ct} [eq. (23)] was introduced and adjusted simultaneously with parameter I upon comparing two different types of first-shell, dihydrated complexes of Zn^{2+}.

—The effective radii on the heteroatoms. The radii of the carbonyl O was adjusted for the Zn^{2+}–formaldehyde complex, with the cation lying in the formaldehyde plane, the Zn—O distance set at 1.8 Å, and four stepwise variations of 30° undertaken on the θ angle C—O—Zn starting from $\theta = 90°$. The so-derived effective radii were actually either equal to or 0.05 Å smaller than those on the hydroxyl oxygen. The effective radii on carboxylate oxygens were calibrated on two types of Zn^{2+}–formate complexes, with Zn^{2+} lying in the formate plane: the so-called bridge complex (B) (see, e.g., refs. 25, 52, and 53), in which Zn^{2+} binds simultaneously to the two anionic oxygens and at equal distances from both. Three stepwise 0.1 Å variations on the Zn—C distances were performed, from 2.1 Å to 2.3 Å; and the so-called external complex (E), in which Zn^{2+} binds one anionic oxygen with the corresponding Zn—O bond trans to the bond linking C to the other O. The Zn—O distance was set at 1.8 Å, and four stepwise variations of the θ angle were performed in 30° steps, from 90° to 180°. For both formaldehyde and formate, the effective radii of the π lone pairs were calibrated by setting Zn^{2+} at 1.8 Å from the bound oxygen and perpendicular to the ligand plane, with $\theta = 120°$. For both carbonyl and carboxylate oxygens, the increments of effective radii of the lone pairs are 0.0 and 0.3 for W and U, respectively. As indicated in the Introduction, the effective radii on the remaining ligands were set to reproduce the radial, in-plane evolutions of E_1(SCF), E_{pol}(SCF), and E_{ct}(SCF) at a fixed θ. Because of penetration effects in the expression of E_c(SCF),[39] identification of E_{MTP}(SMM) and E_c(SCF) is not possible. Rather, as was done in our previous studies,[24,25,49] E_{rep}(SMM) was calibrated in such a way that E_1(SMM) = $E_{MTP} + E_{rep}$ matches E_1(SCF) for these radial variations.

Upon calibrating the thiol Sulfur, we found that a sp^3 hybridization provided highly unsatisfactory radial as well as angular behaviors of E_{rep}(SMM) and E_{ct}(SMM) as compared to the corresponding *ab initio* SCF terms. On the other hand, a representation in terms of one sp hybrid directed along the sulfur's external bisector, and two π hybrids perpendicular to the H—S—C plane through S, yielded a considerably improved agreement to the *ab initio* results, and it is this representation which we will adopt throughout. The increments of effective radii on the thiol sulfur π lone pairs are 0.50 and 0.40 for W and U, respectively.

Finally, to account for the fact that rotations of the cation around a cone centered on the C—O— (alkoxy) or C—S— (thiolate) bonds should not affect numerically the values of E_{rep} and E_{ct} which involve the lone pairs, we have endowed the sp^3 hybridized alkoxy oxygen and thiolate sulfur with six lone pairs (instead of three) but affected each with an occupation number of 1 rather than 2. After several trials bearing on the hydroxy oxygens, we have adopted for this specific oxygen a representation devoid of lone pairs for the expression of E_{rep}, but retaining a six lone pair representation for E_{ct}.

The values of the multiplicative factor C_1 are 243.9 and 487.8 for bond–cation and lone pair–cation terms, respectively. The ratio of 2 between these two values was adopted to account for the presence of 1/sqrt(2) factor in the expansion of a bond orbital on its two centers. The value of the exponent α is 10.88. These values are the same ones as in our joint SCF/SMM study devoted to H-bonded complexes.[28] A complete list of parameters, including the effective radius of Zn^{2+} and the values of the K_{PM} preexponential factors, is given in the Appendix. These values are given for energies expressed in kcal/mol and distances in angstrom.

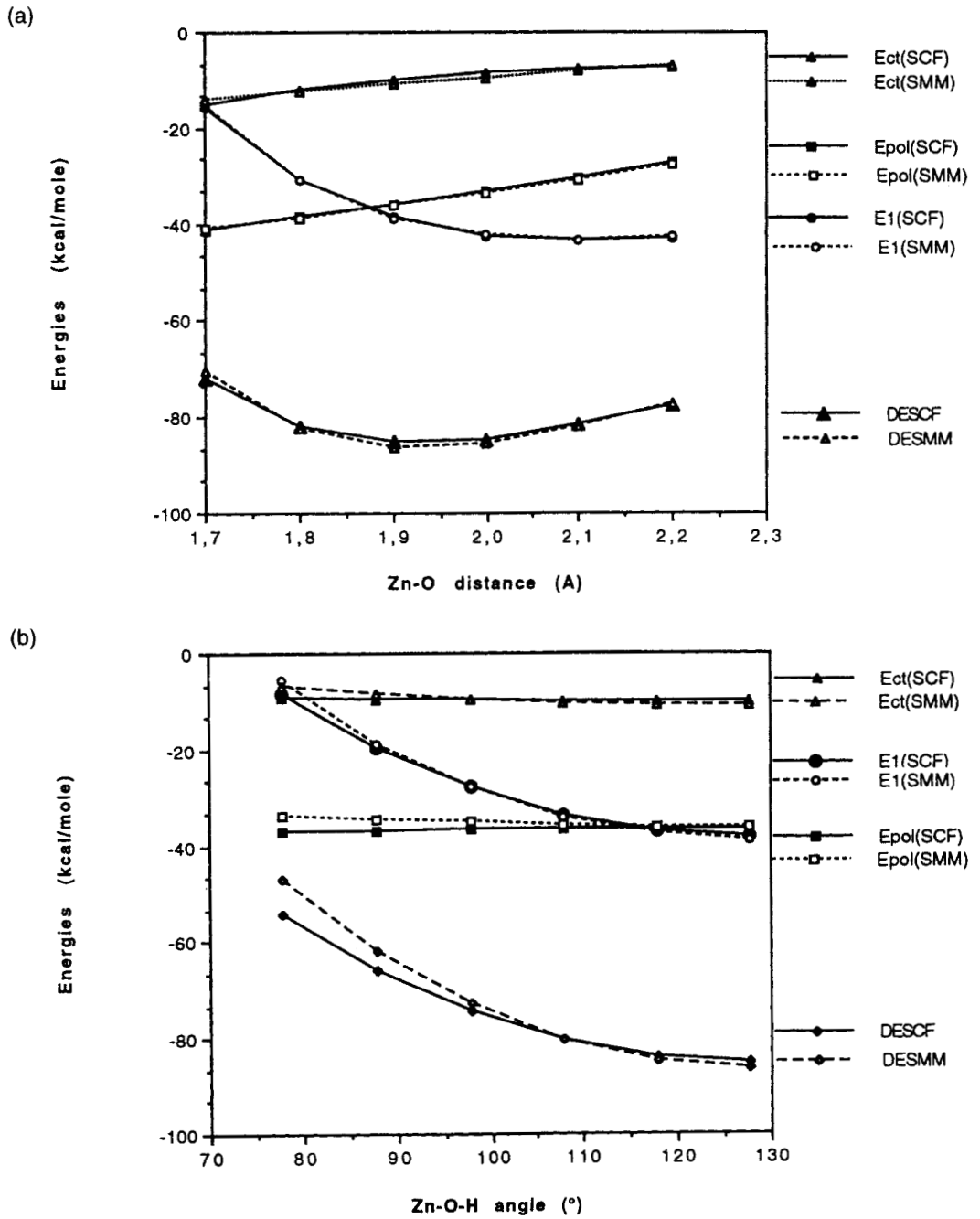

FIGURE 1. Zn^{2+}–water. Evolutions of the SCF and SMM energy terms as a function of (a) in-plane variations of the O—Zn distance and (b) in-plane variation of the θ = H—O—Zn angle. The O—Zn distance is set to 1.9 Å.

Results and Discussion

We wish to compare the behavior of the *ab initio* SCF supermolecule binding energies ΔE(SCF) and their components—Coulomb, E_c; exchange, E_e; first order, $E_1 = E_c + E_e$; polarization, E_{pol}; charge transfer, E_{ct}; and second order, $E_2 = E_{pol} + E_{ct}$—with the corresponding SMM terms: electrostatic multipolar, denoted as E_{MTP}(SMM), short-range repulsion, E_{rep}(SMM), first-order E_1(SMM) = E_{MTP}(SMM) + E_{rep}(SMM), and E_{pol}(SMM), E_{ct}(SMM), as well as E_2(SMM). The results of our computations are reported in Tables I–VIII. For conciseness, several tables of results are available only as supplementary material (available upon request from the author). They will be labeled with an asterisk throughout. A detailed discussion of the *ab initio* SCF results with the RVS decomposition was provided in our previous article,[17] and we will focus here on the behavior of the SMM energy terms in relation to these.

We will present first the results of the complexes of Zn^{2+} with water, on which most of the calibration effort bore. We will then present the results on the complexes of Zn^{2+} with its three neutral ligands—formamide, imidazole, and methanethiol—and then present those with its anionic ones in the order formate, hydroxy, and methanethiolate.

Zn^{2+}–WATER

Table IA* and Figure 1a report the evolutions of ΔE, E_1, E_{pol}, and E_{ct} as a function of the Zn—O distance, with Zn^{2+} lying along the external bisector in the plane of water. For the preset Zn—O distance of 1.9 Å, Figure 1b compares their dependencies as a function of in-plane variations of the angle $\theta = H_1—O—Zn$. Out-of-plane displacements of Zn^{2+} in the bisecting plane were also investigated (unpublished).

The calibration of E_{rep}(SMM) enables the numerical values and corresponding radial behavior of E_1(SMM) to match closely those of E_1(SCF). A similar good match is obtained, within E_2, for E_{pol}(SMM) versus E_{pol}(SCF). This is achieved through the complex radial behavior imposed on E_{pol}(SMM) by the S(A, M) function screening the field. Increasing the cation–ligand separation reduces the magnitude of the unscreened polarizing field, but this is counteracted by the corresponding decrease of S. Computations that did not resort to an iterative procedure resulted in too fast a decrease of E_{pol} for the longer Zn—O distances (unpublished data). With the present formulation and calibration of E_{ct}, the radial behavior of E_{ct}(SMM) term does not reproduce E_{ct}(SCF) as accurately. It nevertheless permits us to reproduce the SCF value to within 1.0 kcal/mol for d(Zn—O) equal to 1.7 Å and beyond.

Figure 1b shows that decreasing θ results in a

TABLE II.
Zn^{2+}–Formamide: Comparison between the SCF / RVS and SMM Binding Energies as a Function of Variations of the θ = C=O—Zn Angle.

θ	120°	135°	150°	165°	180°	195°	210°	225°	240°
ΔE(SCF)	−124.2	−128.2	−128.4	−127.0	−126.0	−125.1	−125.2	−121.7	−113.8
E_c	−85.3	−88.1	−88.1	−87.0	−86.2	−85.5	−84.4	−81.7	−74.4
E_e	26.3	23.7	21.7	20.5	20.3	20.8	22.2	24.6	27.8
E_1	−59.0	−64.4	−66.4	−66.5	−65.9	−64.6	−62.6	−57.1	−46.7
E_{pol}	−51.8	−52.0	−51.9	−51.6	−51.5	−51.4	−51.5	−51.6	−52.4
E_{ct}	−13.4	−11.8	−10.1	−8.9	−8.6	−9.5	−11.1	−13.0	−14.7
E_2	−65.2	−63.8	−62.0	−60.5	−60.1	−60.5	−62.6	−64.6	−67.1
ΔE(SMM)	−124.0	−129.1	−128.1	−125.8	−123.5	−122.4	−122.0	−119.5	−111.7
E_{MTP}	−80.0	−82.8	−81.7	−79.4	−77.6	−76.9	−76.8	−75.1	−68.7
E_{rep}	16.7	14.7	13.1	11.9	11.5	11.9	13.1	14.9	17.3
E_1	−63.3	−68.0	−68.6	−67.5	−66.1	−65.0	−63.6	−60.2	−51.4
E_{pol}	−47.3	−48.7	−49.9	−50.4	−50.2	−49.5	−48.2	−46.9	−46.5
E_{ct}	−13.3	−12.1	−9.9	−7.9	−7.2	−7.9	−10.1	−12.4	−13.8
E_2	−60.6	−61.1	−59.5	−58.3	−57.4	−57.4	−58.3	−59.3	−60.3

Energies in kcal / mol, angles in degrees.

progressive loss of the binding energy, becoming severe (> 19 kcal/mol) 40° away from the external bisector. The progressive loss of ΔE(SCF) upon decreasing θ reflects the behavior of E_1(SCF), itself dominated by the corresponding behavior of E_c(SCF). The numerical values of E_1(SMM) match closely those of E_1(SCF) for $\theta > 85°$. E_{pol}(SCF) remains virtually insensitive to θ decreases, and E_{ct}(SCF) diminishes by a small amount (0.5 kcal/mol) within this range, with the two corresponding SMM terms diminishing there in concert, each by a modest amount. E_2(SMM) matches E_2(SCF) to within 1.4 kcal/mol in this interval.

Zn^{2+}–FORMAMIDE

Computations for Zn^{2+}–formaldehyde (available upon request) and Zn^{2+}–formamide provide the first test of the transferability of the various equations that were adjusted to the Zn^{2+}–water case. The comparisons between the SCF and SMM procedures will be reported here for the preset Zn—O distance of 2.0 Å. Table II lists the evolutions of the SCF and SMM interaction energies as a function of in-plane variations of the θ = C—O—Zn angle at a prefixed O—Zn distance of 2.0 Å, starting from $\theta = 90°$, with the O—Zn segment cis to the C—H bond (values of $\theta > 180°$ correspond to the O—Zn segment cis to the amine group). Figure 2 compares the evolutions of relevant SCF and SMM energy terms as a function of the angle ϕ = H—C=O—Zn, with the Zn—O distance and the θ angle being set at 2.0 Å and 135°, respectively.

Table II shows the best value of ΔE(SCF) to occur at $\theta = 150°$. This is also the case with ΔE(SMM), which is able to match it to within 2.7 kcal/mol out of 120 over the whole range of θ values investigated. The best value of E_1(SCF) is found between 150° and 165°, and that of E_1(SMM) at 150°. Starting from the value of 180°, E_e(SCF) and E_{rep}(SMM) start to increase regularly upon varying θ, whereas the best values of E_c(SCF) and E_{MTP}(SMM) are at 135°. Similar to the Zn^{2+}–water and Zn^{2+}–formaldehyde cases (unpublished results), the angular preference of E_{MTP}(SMM) originates from its charge quadrupole component, overcoming the preference in favor of $\theta = 180°$ set by the summed charge–charge and charge–dipole terms. E_{pol}(SCF) is very shallow over the whole range of values explored. The behavior of E_{pol}(SMM) is more accented, with its maximum at $\theta = 165°$ and its smallest value, 3.9 kcal/mol out of 50 above it, at $\theta = 240°$. Both E_{ct}(SCF) and E_{ct}(SMM) have their best values at $\theta = 120°$ and $\theta = 240°$—namely, when the cation lies along the direction of an sp^2 lone pair orbital of the carbonyl oxygen and their numerical values are close.

Figure 2 shows that rotating Zn^{2+} along a cone away from the formamide plane is prejudicial to

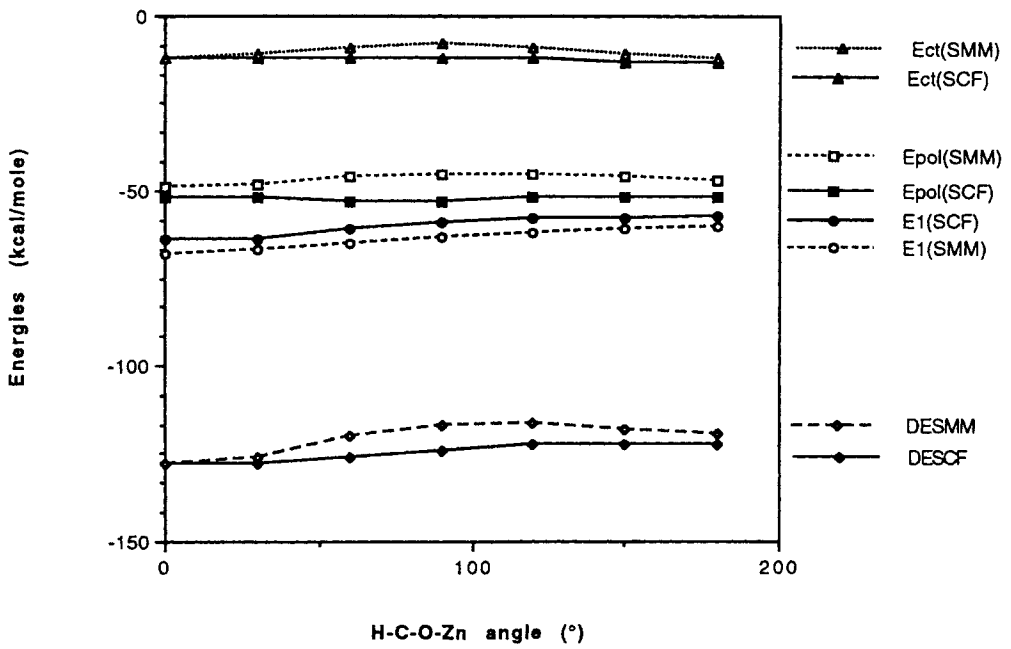

FIGURE 2. Zn^{2+}–formamide. Evolutions of the SCF and SMM energy terms as a function of out-of-plane variations of the ϕ = H—C—O—Zn angle. The O—Zn distance is set to 2.0 Å, and the θ = C—O—Zn angle is set to 135°.

the binding energy, due principally to the loss incurred on E_1. The two extreme values of E_1(SCF), for an in-plane location of Zn^{2+}, cis and trans to the C—H bond, are separated by 7.3 kcal/mol, a difference closely accounted for by the corresponding SMM difference of 7.8 kcal/mol. E_{pol}(SCF) displays a shallow behavior over the whole range of ϕ values, with its best value, 0.9 kcal/mol larger than at $\phi = 0°$, being found for $\phi = 90°$ (i.e., perpendicular to the formamide plane). This is not the case with E_{pol}(SMM), which is 3.4 kcal/mol weaker at $\phi = 90°$ than at $\phi = 0°$. In contrast to its in-plane angular behavior, E_{ct}(SCF) is virtually insensitive to variations of ϕ except for the two largest values, with E_{ct}(SMM) behaving in a slightly more accented way. The presence of a π-bonding orbital on the carbonyl oxygen appears necessary to ensure a smooth decrease of

TABLE IIIA.
Zn^{2+}–Imidazole: Comparison of the SCF / RVS and SMM Binding Energies as a Function of the θ = C—N—Zn Angle.

θ	98°	108°	118°	128°	138°	148°	158°
ΔE(SCF)	−136.9	−143.1	−147.0	−148.0	−145.8	−140.5	−132.0
E_c	−95.1	−105.6	−112.0	−114.0	−111.4	−104.2	−92.7
E_e	52.9	55.0	56.7	57.4	57.1	56.1	54.6
E_1	−42.2	−50.5	−55.3	−56.5	−54.3	−48.1	−38.1
E_{pol}	−75.1	−71.8	−70.8	−69.5	−69.5	−70.5	−73.2
E_{ct}	−19.6	−20.9	−21.6	−22.0	−22.1	−21.8	−20.7
E_2	−94.7	−92.7	−91.7	−91.5	−91.6	−92.3	−93.9
ΔE(SMM)	−130.6	−140.5	−146.8	−149.8	−149.4	−145.3	−136.7
E_{MTP}	−76.2	−85.1	−91.0	−93.9	−93.6	−89.9	−83.0
E_{rep}	34.6	34.8	35.6	36.3	36.8	37.5	39.9
E_1	−41.7	−50.3	−55.4	−57.6	−56.8	−52.4	−43.1
E_{pol}	−71.1	−70.1	−69.9	−70.2	−71.2	−73.1	−76.3
E_{ct}	−17.8	−20.1	−21.5	−22.0	−21.4	−19.8	−17.3
E_2	−88.9	−90.2	−91.4	−92.2	−92.6	−92.9	−93.6

The N—Zn distance is set at 1.9 Å. Energies in kcal / mol, angles in degrees.

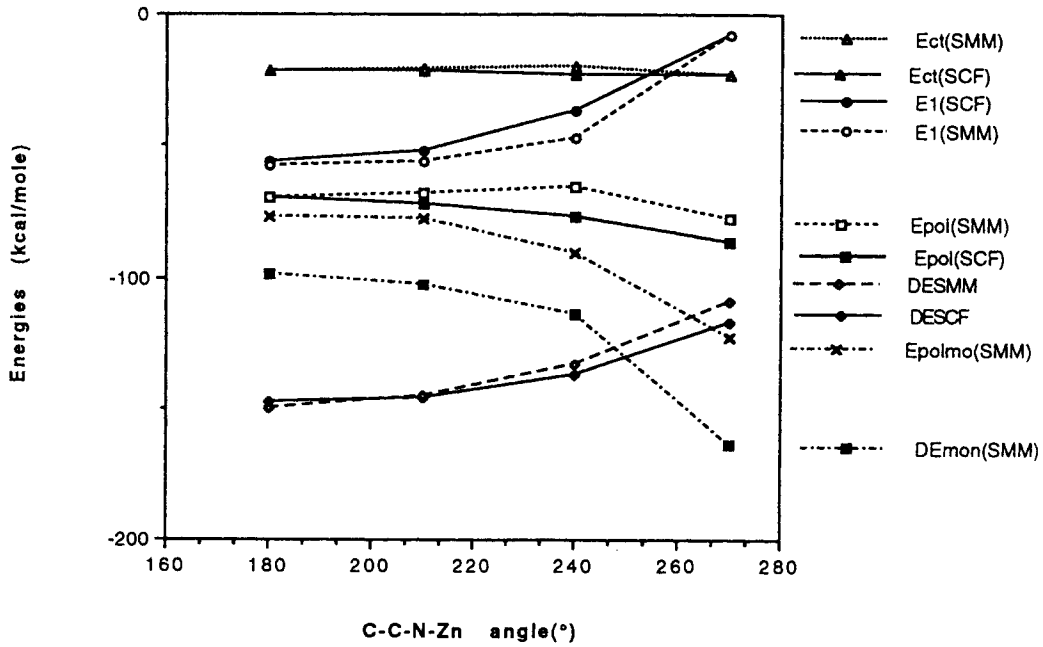

FIGURE 3. Zn^{2+}–imidazole. Evolutions of the SCF and SMM energy terms as a function of out-of-plane variations of the ϕ = C—C—N—Zn angle. The N—Zn distance is set to 1.9 Å.

E_{ct}(SMM), because its attractive effect will be felt progressively upon Zn^{2+} leaving the formamide plane, thereby compensating for the steep corresponding decrease of the attraction contributed by one sp^2 lone pair orbital.

ΔE(SMM) is able to match ΔE(SCF) to within 3.5 kcal/mol out of 120, except when ϕ is in the range 60°–120° (i.e., close to the perpendicular to the ligand plane, where the misfit can reach 7 kcal/mol).

Zn^{2+}–IMIDAZOLE

Table IIIA reports the evolution of the SCF and SMM binding energetics as a function of in-plane variations of the $C_2—N_3—Zn$ angle, with the N—Zn distance being set at 1.9 Å. With Zn^{2+} along the external bisector and the N—Zn distance set at 1.9 Å, Table IIIB* and Figure 3 report the evolution of the binding energetics as a function of 30° variations of the dihedral angle ϕ = $C_4—C_2—N—Zn$.

Tables III(A–B*) show the second-order term, E_2, to provide an even more prominent contribution to the binding energies than with the O-containing ligands. Within E_2, the value of E_{ct} at equilibrium, amounting to −22 kcal/mol, is comparable to the one computed in the Zn^{2+}–formate bidentate complex at equilibrium—namely, −25 kcal/mol—and twice the corresponding value computed in the Zn^{2+}–water one.

Table IIIA shows that excursions of more than 30° away from the external bisector result in significant (> 10 kcal/mol) losses in the binding energy. The best value of E_1(SCF) is found at θ = 128°, and this preference is imposed by E_c, whereas E_e decreases upon varying θ by an amplitude of up to 30°. These trends can be well accounted for by E_1(SMM) and its two components, E_{MTP} and E_{rep}, with the decrease of the latter corresponding to the decrease of the cation-N-centered *sp* lone pair repulsion: Such an effect is more important than the corresponding increase of the Zn^{2+} repulsion with an N—C bond. Whereas E_1(SMM) matches E_1(SCF) to within 1 kcal/mol out of 40 upon decreasing θ from 128° to 98°, the numerical agreement is less satisfactory upon increasing it to θ = 158°. This is essentially due to a slower corresponding decrease of E_{MTP}(SMM) than that of E_c(SCF). We have recomputed the Zn^{2+}–imidazole multipolar interaction energy by taking into account explicitly the charge–octupole interaction within E_{MTP}(SMM), because this term is not incorporated in the present version of the SMM program. For that purpose, the multipolar expansion of imidazole was derived from the Stone analysis[54] instead of the Vigné-Maeder-Claverie one.[31] Incorporation of this term with the help of a specific code (W. J. Stevens, Center for Advanced Research in Biotechnology, unpublished) yielded an improved numerical match in the compared evolutions of E_{MTP}(SMM) versus E_c(SCF). This implies that the explicit introduction of octupoles for aromatic systems whose MOs are computed with large basis sets and polarization functions can be envisaged as an additional future improvement of the SMM procedure through its E_{MTP} term. However, for all other Zn^{2+}–ligand complexes investigated so far, our standard multipolar expansion limited to quadrupoles did ensure a satisfactory numerical match between E_1(SCF), and E_1(SMM), as will be shown in the case of the Zn^{2+} complexes with the succeeding ligands.

E_{pol}(SCF) increases by up to 6 kcal/mol out of 70 upon varying θ by an amplitude of 30°, whereas E_{ct}(SCF) decreases in concert, by a smaller amount (< 2.4 kcal/mol out of 20). Both trends are correctly accounted for by the corresponding E_{pol}(SMM) and E_{ct}(SMM) terms.

In view of large-scale simulations of polyligated complexes of Zn^{2+} involving imidazole(s) and a complete relaxation of the Zn^{2+} position, it was essential to assess the robustness of the SMM procedure upon dealing with out-of-plane displacements of the Zn^{2+} position around its ligating nitrogen. For such nonplanar positions, critical issues pertain to the proper angular dependencies of the electrostatic terms—namely, E_{MTP}(SMM) limited to quadrupoles, and E_{pol}(SMM) using our set of localized, anisotropic polarizabilities—as well as to those of the short-range ones—namely, E_{rep}(SMM) and E_{ct}(SMM), which use an explicit, localized representation of the π lone pairs. For that purpose we have performed stepwise out-of-plane displacements of Zn^{2+} bisecting the C—N—C angle with the N—Zn distance being set at 1.9 Å (see Fig. 3). We observe that up to $\Delta\phi$ = 60° [at which position ΔE(SCF) is 11 kcal/mol less favorable than at the in-plane position], ΔE(SMM) can still match ΔE(SCF) to within 2 kcal/mol out of 137. ΔE(SCF) is considerably (31 kcal/mol) weaker upon reaching the perpendicular to the imidazole plane, so that the corresponding position is no longer energetically relevant. ΔE(SMM) there matches ΔE(SCF) to within 4 kcal/mol out of 117. Over the range of ϕ values

investigated, E_1(SMM) matches E_1(SCF) satisfactorily, except when $\Delta\phi = 60°$, where it is 10 kcal/mol larger. Within E_1(SMM), the decrease of E_{MTP} is slower than that of E_c(SCF), on account of the absence of the charge–octupole term. The shallow behavor of E_{rep}(SMM) up to $\Delta\phi = 60°$ and its steep increase when $\phi = 270°$ are due to the fact that upon moving Zn^{2+} away from the imidazole plane, the Zn^{2+}–*sp* nitrogen lone pair repulsion decreases, until the *z* lobe is encountered (i.e., when $\phi = 270°$), resulting in a strong cation–lone pair repulsion. It is instructive to observe in this respect that E_e(SCF) also starts to decrease when $\Delta\phi = 30°$, is shallow in the $\Delta\phi$ interval of 30° to 60°, and undergoes a fast increase at $\phi = 270°$ (Table IIIB*).

E_{ct}(SCF) has an extremely shallow behavior over the range of ϕ values explored, being actually slightly larger (0.6 kcal/mol) at $\phi = 270°$ than in plane. E_{ct}(SMM) slowly decreases (by 2.4 kcal/mol out of 20) until $\Delta\phi = 60°$, and it increases again when $\phi = 270°$. A modest preference (1.4 kcal/mol out of 24) is found in favor of $\phi = 270°$ over $\phi = 180°$. E_{pol}(SCF) increases regularly up to $\phi = 270°$. On the other hand, E_{pol}(SMM) undergoes a small (4 kcal/mol out of 70) decrease from $\phi = 180°$ to $\phi = 240°$ but increases again when $\phi = 270°$.

In marked contrast to the strong preference of E_{MTP} in favor of the in-plane position of Zn^{2+} rather than the perpendicular one (−94 versus −60 kcal/mol, respectively), the sole monopole–monopole term was seen to manifest a nearly equally strong (30 kcal/mol out of 67) inverse angular preference. This can be understood by the fact that upon undergoing out-of-plane variations at a fixed distance to the ligating *N*, the cation is shifted progressively away from the two hydrogens connected to C_2 and C_4 and undergoes an increasingly reduced charge–charge electrostatic repulsion with them until it reaches the perpendicular. For this position, furthermore, it undergoes more favorable interactions with the imidazole carbons, which bear net partial negative point charges. As such, a truncation of E_{MTP} to its sole monopole–monopole component would have given rise to an approximately 30 kcal/mol preference favoring $\phi = 270°$ over $\phi = 180°$. Such a result underlines the necessity of a representation of the electrostatic term with higher-than-monopole terms and the fact that simplified molecular mechanics force fields can give rise to severe erroneous out-of-plane preferences. A preference for $\phi = 270°$ was indeed observed in molecular mechanics computations on Zn^{2+}–imidazole using standard force fields (D. R. Garmer, private communication).

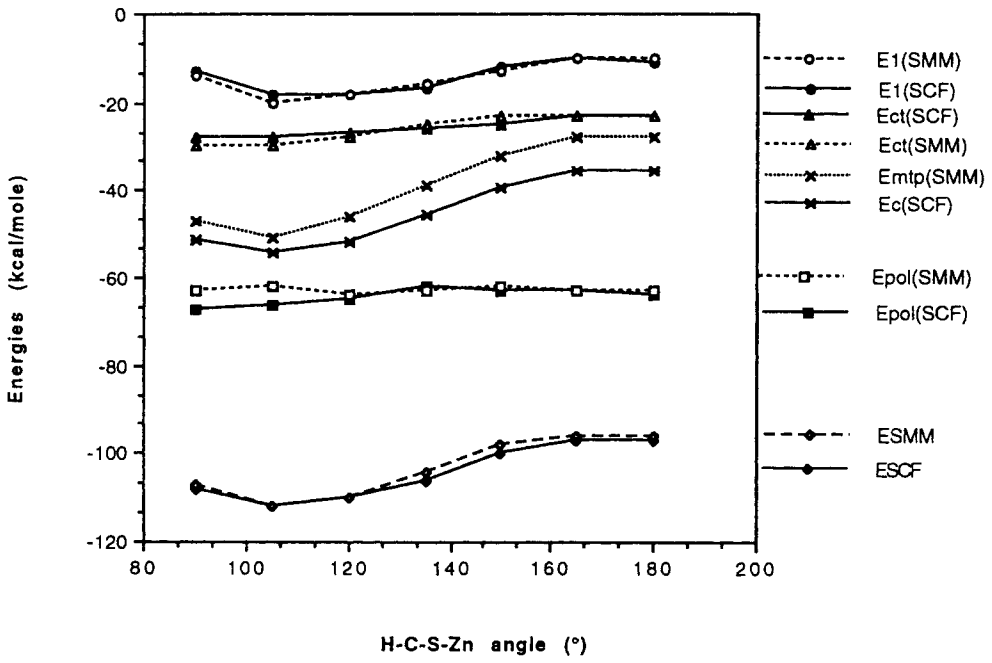

FIGURE 4. Zn^{2+}–methanethiol. Evolutions of the SCF and SMM energy terms as a function of out-of-plane variations of the ϕ = H—C—S—Zn angle. The S—Zn distance is set to 2.4 Å.

We have also reported the behavior of E_{pol}(SMM) as would be computed with unscreened, isotropic polarizabilities. Comparing again the two extreme values of $\phi = 180°$ and 270°, we observe an even more dramatic preference of E_{pol}, amounting to 46 kcal/mol and favoring the perpendicular position over the planar one (−123 versus −77 kcal/mol, respectively). By contrast, the corresponding increase of E_{pol}(SCF) is limited to 18 kcal/mol. Such a result indicates that incorporating an explicit polarization term, as is frequently done to refine existing molecular mechanics force fields (see e.g., refs. 55–59), necessitates appropriately accounting for screening as well as nonisotropic effects and confronting the value of this term to its *ab initio* counterpart in test cases.

Zn^{2+}–METHANETHIOL

Table IV* and Figure 4 report the evolutions of the SCF and SMM binding energies as a function of out-of-plane variations of the position of Zn^{2+}, at a fixed distance of 2.4 Å, with Zn^{2+} remaining on the external bisector. In marked contrast with the imidazole complex, in-plane locations of Zn^{2+} correspond to much less favorable values of the binding energies than out-of-plane ones. We observe a remarkable preference of both ΔE(SCF) and ΔE(SMM) for the value of $\phi = 105°$—namely, when Zn^{2+} is close to the perpendicular to the H—S—C plane. ΔE(SMM) is able to match ΔE(SCF) to within 2.2 kcal/mol out of 100 over the whole range of ϕ values covered here. Within E_1(SCF), this preference is imposed by E_c(SCF), which is 18.9 kcal/mol more favorable at $\phi = 105°$ than at $\phi = 180°$. It can be accounted for by the E_{MTP}(SMM) term, with the corresponding preference amounting to 23.3 kcal/mol and originating from the charge–quadrupole term. The angular preferences set by the electrostatic terms are strongly opposed by the short-range repulsion energies, as evidenced by the much shallower character of the E_1 minima than of the E_c and E_{MTP} ones. Within E_2, this preference is imposed by E_{ct}(SCF), contributing an additional 5 kcal/mol in favor of $\phi = 105°$ over $\phi = 180°$, and has its pendant in terms of E_{ct}(SMM). It is noteworthy that even though E_{pol} is the dominant contributor to the total binding energy, it has a shallow behavior over the whole range of explored ϕ values, increasing from $\phi = 180°$ to $\phi = 105°$ by less than 2 kcal/mol out of 60 in both SCF and SMM computations. A preference of Zn^{2+} for an out-of-plane location was noted by Pullman and co-workers in

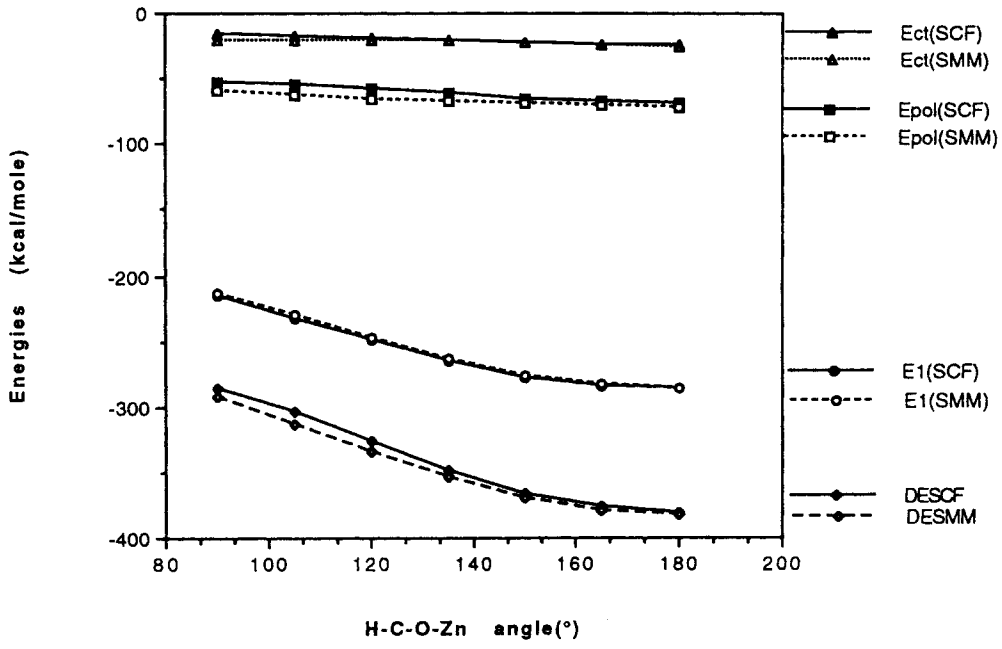

FIGURE 5. Zn^{2+}–formate in the bidentate mode. Evolutions of the SCF and SMM energy terms as a function of out-of-plane variations of the τ = H—C—O—Zn angle. The C—Zn distance is set to 2.2 Å.

their studies of the complex between Zn^{2+} and H_2S.[10]

Zn^{2+}–FORMATE

The interaction of Zn^{2+} with formate provides an extreme test of the functional forms and concomitant parameters developed for the SMM procedure. The anionic nature of formate can be expected to exaggerate the Coulombic, polarization, and charge transfer components of the interaction energy. Also, the delocalized nature of the anionic charge can introduce complications related to charge localization at monodentate binding geometries. However, these effects were found to be less severe than anticipated, as discussed later.

To sample the interaction energy surface for Zn^{2+} binding, we have considered three distinct geometrical configurations:

—*Out-of-plane, bidentate mode.* The Zn—C distance is held at its in-plane optimized value. With Zn^{2+} remaining equidistant from the two anionic oxygens, the dihedral angle τ = (H—C—O—Zn) is decreased by 15° steps, from $\tau = 180°$ (in plane) to $\tau = 90°$ (for which value the Zn—C bond is perpendicular to the formate plane).

—*In-plane monodentate binding.* The Zn—O distance is set to 2.0 Å (a distance not used for the calibration), and, similar to the formaldehyde complex, the θ angle (C—O—Zn) is varied by 30° increments, from $\theta = 90°$ to $\theta = 180°$. (Additional results for $d_{Zn-O} = 1.8$ and 2.2 Å are available from the author upon request).

—*Out-of-plane, monodentate binding.* Again as in the formaldehyde complex, the Zn—O distance is set at 2.0 Å, the θ angle is held at 120°, and Zn^{2+} is rotated by 30° increments of the ϕ dihedral angle on a cone having the CO bond as an axis.

Bidentate Binding Mode

Figure 5 shows that small excursions of Zn^{2+} out of the formate plane substantially reduce the binding energy. A loss of 14.5 kcal/mol thus occurs when $\tau = 150°$, and of 32 kcal/mol when $\tau = 135°$. E_1(SMM) matches E_1(SCF) to within an accuracy of < 1.3 kcal/mol (i.e., of 0.5% until τ equals 135°). The values of E_{pol}(SMM) are overestimated with respect to those of E_{pol}(SCF). For the best value of $\tau = 180°$, such an overestimation amounts to 3 kcal/mol out of 69, and this is the least successful feature of our SMM representation of the bidentate Zn^{2+}–formate complex. E_{ct}(SMM), on the other hand, reproduces closely E_{ct}(SCF),

TABLE VA.
Zn^{2+}–Formate in the Monodentate Position: Comparison between the SCF / RVS and SMM Energies as a Function of In-Plane Variations of the θ = C—O—Zn^{2+} Angle.

θ	90°	120°	150°	180°
ΔE(SCF)	−310.2	−321.3	−318.9	−317.1
E_c	−269.0	−277.6	−273.5	−272.1
E_e	40.1	32.6	26.8	24.1
E_1	−228.9	−245.0	−246.7	−248.0
E_{pol}	−58.6	−53.0	−53.3	−53.0
E_{ct}	−22.8	−23.2	−18.9	−16.1
E_2	−81.4	−76.2	−72.2	−69.1
ΔE(SMM)	−301.9	−321.4	−319.3	−317.3
E_{MTP}	−263.1	−270.4	−265.7	−263.8
E_{rep}	30.3	17.2	13.4	11.8
E_1	−232.8	−253.2	−252.2	−252.0
E_{pol}	−50.4	−46.6	−49.6	−51.4
E_{ct}	−18.7	−21.7	−17.4	−13.8
E_2	−69.1	−68.3	−67.0	−65.2

The dZn—O distance is set at 2.0 Å. Energies in kcal / mol, angles in degrees.

both in terms of numerical values and in terms of angular dependence upon τ.

In-Plane Monodentate Binding

The SCF and SMM interaction energies are compared in Table VA. We first observe that upon passing from $\theta = 120°$ to $\theta = 180°$, E_c(SCF) has diminished by an amount of 5.5 kcal/mol. This result is similar to the corresponding one obtained with formaldehyde and is all the more surprising here because, upon increasing θ, Zn^{2+} moves progressively closer to the second anionic oxygen, toward the zone in which the maximum of the negative formate charge lies. Once again, this trend of E_c(SCF) is reproduced by E_{MTP}(SMM). Examination of the different components of the latter reveals that while both charge–charge and charge–dipole terms increase from $\theta = 120°$ to $\theta = 180°$ (−252.0 versus −257.8 kcal/mol and −4.7 versus −20.8 kcal/mol, respectively), the charge–quadrupole term, which is attractive at $\theta = 120°$ (−13.5 kcal/mol), becomes repulsive at $\theta = 180°$ (14.8 kcal/mol). The total E_c(SMM) term then favors $\theta = 120°$, which may be contrary to common intuition. These findings, for which (besides the SCF results reported in refs. 17 and 18) there seems to be no precedent reported for cation–anionic ligand interactions, indicate that even in a highly ionic complex such as Zn^{2+}–formate, for which the charge–charge term is numerically overwhelming, a complete multipolar expansion (encompassing quadrupoles or quadrupole-fitted monopoles and dipoles) to compute the electrostatic term is necessary and that such an expansion ought to be derived from a high-quality basis set. The short-range repulsive energy contribution is significantly larger for $\theta = 120°$ than for $\theta = 180°$ (by 8.5 and 5.4 kcal/mol in the SCF and SMM computations, respectively). With our present formulation, it is the cation–lone pair term that dominates the E_{rep}(SMM) variations (15.8 kcal/mol at $\theta = 120°$ versus 11.7 at $\theta = 180°$), which highlights the necessity of an anisotropic character in its formulation. The mutual compensation between electrostatic and short-range repulsion results in E_1 having a very flat angular character in the range 120°–180°. As θ increases from 120° to 180°, E_{pol}(SCF) remains virtually constant, whereas E_{pol}(SMM) increases progressively. Similar to the Zn^{2+}–formaldehyde complex, the numerical agreement between E_{pol}(SCF) and E_{pol}(SMM) is best at the collinear geometry. Comparing the present results with those published in ref. 25 for divalent metal complexes of formate, which resorted to isotropic polarizabilities and in which a monotonous decrease of E_{pol}(SMM) was observed upon increasing θ, demonstrates that the use of anisotropic polarizabilities provides an important improvement in the representation of E_{pol}. Similar to E_{ct}(SCF), E_{ct}(SMM) favors $\theta = 120°$ when Zn^{2+} lies along the direction of one sp^2 lone pair of the anionic oxygen.

Out-of-Plane Monodentate Binding

Out-of-plane configurations were investigated with the Zn—O—C angle fixed at 120° (see Table VB). E_1(SMM) matches E_1(SCF) with an accuracy of < 8.5 kcal/mol out of approximately 253 (i.e., $< 3.5\%$), comparable to the one obtained in the energetically relevant in-plane and bidentate configurations investigated earlier. Upon increasing ϕ to 90°, E_{pol}(SCF) increases slightly and decreases past 90°, so its values are very close for the two extreme values of ϕ, 0° and 180° (−53. and −52.8 kcal/mol, respectively). We are unable to account for such a behavior in terms of E_{pol}(SMM). The latter actually decreases by 2.3 kcal/mol when ϕ reaches 90° and is enhanced past this value, resulting in a 3.9 kcal/mol energy difference favoring $\phi = 180°$ over $\phi = 0°$. E_{ct}(SCF) behaves in a significantly more isotropic fashion than was the case with the formaldehyde complex, and this is also the case with E_{ct}(SMM). The former, however, favors $\phi = 0°$ over $\phi = 180°$ by a small amount (0.7 kcal/mol out of 22), whereas an inverse preference by the same amount is found with E_{ct}(SMM). ΔE(SMM) matches ΔE(SCF) to within 3.5 kcal/mol out 300, except when $\phi = 60°$ and 90°, where it is 6.5 kcal/mol smaller. Overall, the large SCF energy variation upon passing from the mono- to the bidentate configurations is correctly accounted for by the SMM computations.

Zn^{2+}–HYDROXY

Zn^{2+}-mediated deprotonation of one water molecule was first predicted to occur in the active site of carbonic anhydrase by Demoulin and Pullman,[9] with a Zn^{2+}–OH complex being formed in the first ligation shell of Zn^{2+} during the formation of a transition state, and possibly also in the stabilization of enzyme active site—Zn^{2+} inhibitor–water complexes.[2] In the prospect of simulations involving such a complex within zinc proteases, we report here our comparison of the SCF and SMM binding energies of Zn^{2+}–OH^-. Table

VIA* and Figure 6 compare the evolutions of the SCF and SMM binding energies as a function of the Zn—O distance, with the θ angle H—O—Zn being set at 180°, and Table VIB compares their evolutions as a function of the θ angle, with the Zn—O distance being set at 1.8 Å.

Figure 6 shows that E_{ct}(SMM) is virtually insensitive to distance variations in the 0.6 Å interval of variations covered. A related behavior could be observed for E_{ct}(SCF) past 1.9 Å, as it decreases by only 0.8 kcal/mol out of 20 between 2.0 and 2.3 Å.

Table VIB shows that the best value of θ is again 120°, preferred by 11 kcal/mol out of 400 over θ = 180°. Similar to the formate complex, it is due, within E_1(SCF), to E_c counteracted by E_e, and within E_2(SCF), to E_{ct} counteracted by E_{pol}. E_1 and E_2 contribute, respectively, 7 and 4 kcal/mol to the global energy difference. ΔE(SMM) can still

TABLE VB.
Zn^{2+}–Formate in the Monodentate Position: Comparison of the SCF / RVS and SMM Binding Energies as a Function of Out-of-Plane Variations of the Position of Zn^{2+}, as Measured by the ϕ = H—C—O—Zn Angle.

ϕ	0°	30°	60°	90°	120°	150°	180°
ΔE(SCF)	−321.3	−321.4	−322.1	−324.8	−331.5	−341.0	−345.9
E_c	−277.6	−276.4	−274.6	−276.6	−284.8	−295.5	−300.6
E_e	32.6	31.7	29.6	28.1	28.3	29.4	30.0
E_1	−245.0	−244.7	−245.0	−248.5	−256.5	−266.1	−270.6
E_{pol}	−53.0	−53.4	−53.6	−53.8	−53.3	−52.9	−52.8
E_{ct}	−23.2	−23.3	−23.5	−22.5	−21.7	−22.0	−22.5
E_2	−76.2	−76.7	−77.1	−76.3	−75.0	−74.9	−75.3
ΔE(SMM)	−321.4	−319.1	−316.2	−318.4	−329.0	−342.1	−348.6
E_{MTP}	−270.4	−252.7	−267.3	−269.6	−277.8	−288.2	−293.1
E_{rep}	17.2	16.3	14.9	14.3	14.9	16.3	17.2
E_1	−253.2	−252.7	−252.4	−255.3	−262.9	−271.9	−275.9
E_{pol}	−46.6	−45.8	−44.4	−44.5	−46.5	−49.2	−50.5
E_{ct}	−21.7	−20.7	−19.4	−18.8	−19.7	−21.1	−22.2
E_2	−68.3	−66.5	−63.8	−63.3	−66.2	−70.3	−72.7

The O—Zn distance is set at 2.0 Å, and the θ angle at 120°.
Energies in kcal / mol, angles in degrees.

TABLE VIB.
Zn^{2+}–Hydroxy: Comparison of the SCF / RVS and SMM Binding Energies as a Function of In-Plane Variations of the θ = H—O—Zn Angle.

θ	90°	105°	120°	135°	150°	165°	180°
ΔE(SCF)	−403.2	−409.9	−411.1	−408.8	−404.9	−401.3	−399.9
E_c	−410.2	−412.4	−408.1	−400.5	−392.4	−386.7	−384.7
E_e	86.6	81.9	75.7	69.2	63.8	60.5	59.4
E_1	−323.6	−330.4	−332.5	−331.3	−328.7	−326.3	−325.3
E_{pol}	−43.1	−44.4	−45.6	−47.0	−48.2	−49.0	−49.3
E_{ct}	−36.6	−35.1	−33.0	−30.6	−28.1	−26.1	−25.3
E_2	−79.7	−79.5	−78.6	−77.6	−76.3	−75.1	−74.6
ΔE(SMM)	−382.5	−408.4	−417.2	−415.5	−408.3	−401.2	−398.4
E_{MTP}	−394.3	−396.5	−391.9	−383.2	−373.6	−366.2	−363.5
E_{rep}	76.5	59.6	50.2	44.7	41.6	39.9	39.4
E_1	−317.8	−336.9	−341.8	−338.5	−332.0	−326.3	−324.1
E_{pol}	−41.8	−45.7	−49.3	−52.0	−53.7	−54.6	−54.8
E_{ct}	−23.0	−25.5	−26.2	−25.0	−22.6	−20.3	−19.5
E_2	−64.8	−81.2	−75.5	−77.0	−76.3	−74.9	−74.3

The dO—Zn distance is set at 1.8 Å. Energies in kcal / mol, angles in degrees.

match ΔE(SCF) to within 2%, at least until θ = 105°.

Zn^{2+}–METHANETHIOLATE

Deprotonation of the Cys sidechains to produce the $-CH_2S^-$ terminal moiety occurs in the active site of cysteine protease enzymes.[20] This moiety is also found in the structure of thiorphan and retrothiorphan,[21] which are extremely potent inhibitors of the Zn^{2+} metallopeptidases thermolysin[1] and enkephalinase.[4] A high-resolution X-ray crystallography study of the complexes of these two drugs with thermolysin shows $-CH_2S^-$ bound directly to Zn^{2+} in the active site.[60] These indications have prompted our present study to unravel in detail the binding energetics involved in such an association.

Table VIIA compares the evolutions of the binding energies as a function of the Zn—S distance, with the θ = C—S—Zn angle being set at 180°. Table VIIB* and Figure 7 compare their evolutions as a function of the θ angle, with the S—Zn distance being set at 2.3 Å.

Table VIIA shows that despite the strongly ionic nature of the complex, the contribution of E_2 amounts at equilibrium distance (2.1 Å) to more than one third of the total ΔE. The large individual values of E_{pol} and E_{ct} within E_2 translate the strong polarizability of CH_3S- coupled to its strong electron-donating character. ΔE(SMM) is able to match ΔE(SCF) to within 3 kcal/mol out of 340 in the 2.0 to 2.4 Å range of interatomic distances. E_{ct}(SMM) can match E_{ct}(SCF) to within 2 kcal/mol out of 30 at equilibrium distance and beyond. The latter decreases slowly upon increasing this distance, by 4.7 kcal/mol from d = 2.0 Å to d = 2.3 Å, and it increases beyond. E_{ct}(SMM) has virtually equal values until the equilibrium distance is reached, beyond which it also begins to increase.

In-plane variations of θ (Table VIIB*) give rise to a remarkable, deep minimum at θ = 105°, with ΔE being 45 kcal/mol stronger for this angular value than at θ = 180° in both SCF and SMM procedures. This is in sharp contrast to the Zn^{2+}–hydroxy and Zn^{2+}–methoxy complexes (results for the latter available upon request), in which θ = 120° was favored over θ = 180° by < 11 kcal/mol out of > 380 in the SCF computations. Within ΔE(SCF), such a preference is dictated by both E_1 and E_{ct}, which contribute 30 and 20.7 kcal/mol, respectively, to it. Within E_1, it is imposed by the electrostatic term E_c, favoring θ = 105° over θ = 180° by 57.5 kcal/mol, but counteracted by the short-range repulsion term E_e, which disfavors the smaller θ value by 29 kcal/mol. A

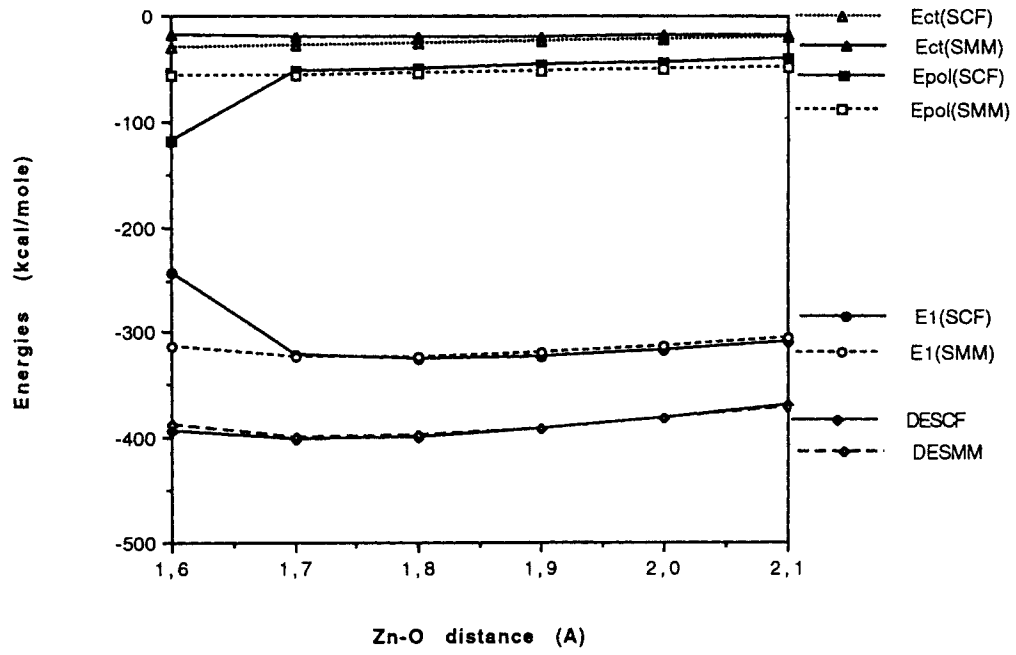

FIGURE 6. Zn^{2+}–hydroxy. Evolutions of the SCF and SMM energy terms as a function of in-plane variations of the O—Zn distance. H, O, and Zn are collinear.

similar balance of effects operates within E_1(SMM). The angular preference of E_{MTP}(SMM) is imposed by the charge–quadrupole term (76 kcal/mol favoring $\theta = 105°$ over $\theta = 180°$), overwhelming the preferences in favor of $\theta = 180°$ set by the summed charge–charge and charge–dipole terms, amounting to 26.4 kcal/mol. This further highlights the crucial need for as complete as possible a multipolar expansion to compute the electrostatic energy term, particularly in highly charged complexes: Such an expansion should encompass up to quadrupoles or quadrupole-fitted monopoles or dipoles. The 49.5 kcal/mol preference of E_{MTP} in favor of $\theta = 105°$ is counteracted by E_{rep}(SMM), which disfavors the smaller θ value by 24 kcal/mol. The origin of the latter difference re-

TABLE VIIA.
Zn^{2+}–Methanethiolate: Comparison of the SCF / RVS and SMM Binding Energies as a Function of the Zn—S Distance.

dZn—S	1.9	2.0	2.1	2.2	2.3	2.4
ΔE(SCF)	−343.9	−351.6	−352.6	−349.3	−343.4	−337.0
E_c	−293.2	−282.4	−272.2	−262.7	−253.8	−245.6
E_e	90.1	63.0	43.8	30.5	21.1	14.7
E_1	203.1	−219.5	−228.4	−232.2	−232.7	−230.9
E_{pol}	−102.1	−96.5	−90.8	−85.4	−79.6	−73.7
E_{ct}	−38.8	−35.8	−33.4	−31.7	−31.1	−32.4
E_2	−140.9	−132.2	−124.2	−117.1	−110.7	−106.7
ΔE(SMM)	−336.6	−348.3	−351.6	−349.4	−344.0	−337.1
E_{MTP}	−286.0	−278.1	−270.0	−262.0	−254.1	−246.4
E_{rep}	85.0	59.0	41.1	28.7	20.0	14.0
E_1	−201.1	−219.1	−228.9	−233.3	−234.1	−232.4
E_{pol}	−104.5	−98.2	−91.5	−84.6	−77.6	−70.8
E_{ct}	−30.9	−30.9	−31.1	−31.5	−32.3	−33.8
E_2	−135.5	−129.1	−122.6	−116.1	−109.9	−104.6

Zn is along the direction of the C—S bond. Energies in kcal / mol, distances in angstroms.

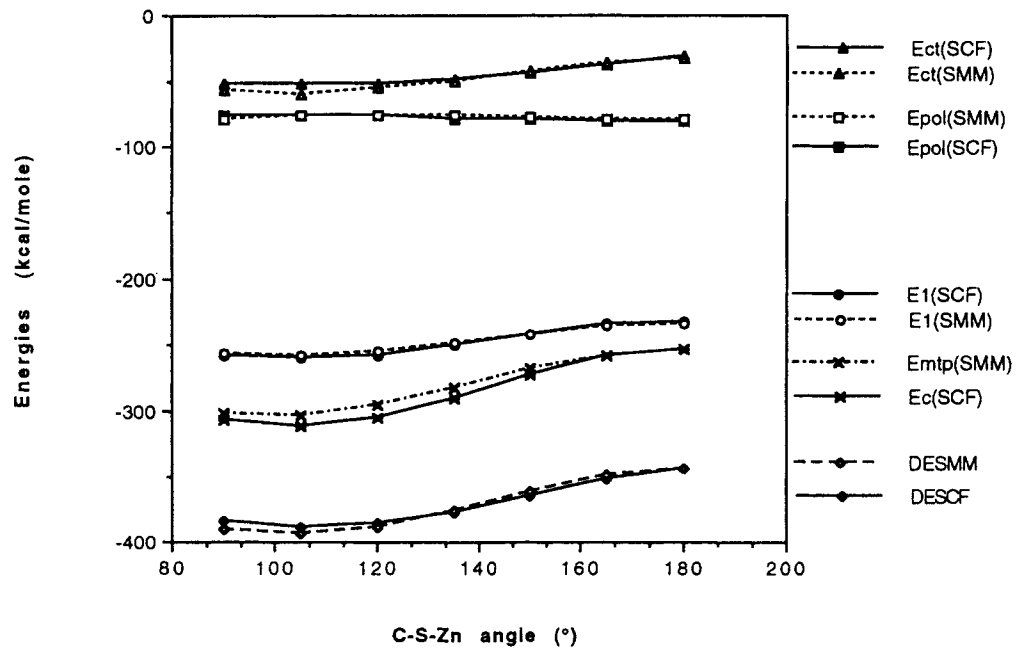

FIGURE 7. Zn^{2+}–methanethiolate. Evolutions of the SCF and SMM energy terms as a function of in-plane variations of the θ = C—S—Zn angle. The S—Zn distance is set to 2.3 Å.

sides virtually exclusively in the lone pair–cation repulsion. Once more, this underlines the need for an anisotropic representation of the short-range repulsion energy around heteroatoms, because it is clear that a pure atom–atom representation would fail to account for the angular behavior of E_e(SCF) outlined here. The shallower angular behaviors of E_1(SCF) and E_1(SMM) compared to those of E_c and E_{MTP} are exemplified in Figure 7. Overall, E_1(SMM) can match E_1(SCF) to within < 3 kcal/mol out of 250.

Within E_2, E_{pol} and E_{ct} again display contrasted angular dependencies. E_{pol}(SCF) and E_{pol}(SMM) are both shallow in the whole angular range covered, with a modest but distinct preference for the larger values of θ, 165° and 180°, and, in the case of E_{pol}(SMM), the smallest one, 90°, as well. It is obvious that a representation of E_{pol} with the help of isotropic polarizabilities[25,44] would fail to account for such an absence of angular character: In that case, E_{pol} would continuously, and strongly, increase upon decreasing θ, due to the increased proximity of the dicationic charge to the polarizable centers of the C—S and C—H barycenters, and incur severe numerical artifacts. The absence of in-plane angular dependency of E_{pol} is due to the balance of two effects: on the one hand, the fact that the amplitude of induced dipoles on the C—S bond and on the average of the three S lone pairs is maximal at $\theta = 180°$, and, on the other hand, the fact that the proximity of Zn^{2+} to the C—S and C—H bond barycenters is optimal for the smallest values of θ; it occurs at $\theta = 105°$ for one of the S-centered lone pair polarizabilities. This leads to an instructive paradox: A representation of E_{pol} with the help of anisotropic polarizabilities alone can account for its isotropic angular character when present. Both E_{ct}(SCF) and E_{ct}(SMM) have their best values at $\theta = 105°$, close to the direction of an sp^3 S lone pair. The SCF and SMM values of -51.8 and -56 kcal/mol are the largest ones we have computed so far for a charge transfer term. The 21 out of 50 kcal/mol angular energy preference of E_{ct}(SCF) is considerably larger than the corresponding ones computed in the formate (6 kcal/mol out of 25), in the formamide (5 kcal/mol out of 13), and in the methoxy complexes (10 kcal/mol out of 30). Such a strong angularity of E_{ct}(SCF) is reproduced by E_{ct}(SMM) (23.5 kcal/mol out of 56). This enhanced angular behavior occurs in spite of the 0.4 Å larger Zn—S than Zn—O distances.

As a result of the close numerical reproduction by each of the SMM terms, E_1, E_{pol}, and E_{ct}, of their SCF counterparts, ΔE(SMM) is able to reproduce ΔE(SCF) to within < 4 kcal/mol out of 380. The preferential value of θ of 105° is supported by the high-resolution X-ray crystal structure of the complex of thiorphan in the active site of thermolysin, where the C—S—Zn angle has a closely similar value, namely 125°.[60]

Di- AND POLYLIGATED COMPLEXES OF Zn^{2+}

The onset of polyligand many-body effects upon di- or polyligation of cationic species[61-63] is a major challenge for molecular mechanics, and these effects are particularly exacerbated with divalent[61] and *a fortiori* trivalent cations.[62] They are most thoroughly documented with water as a ligand. Attempts to represent them so far have resorted to an explicit polarization term[64,65] coexisting with an extraneous term, which for most common representations is a product of three exponentials involving three interacting atoms at a time (e.g., the cation nucleus and a pair of two water oxygen atoms). A critical issue in the present study pertains to whether our molecular mechanics formulation of E_{pol} and E_{ct} produces the correct nonadditive behavior in polyligated complexes of Zn^{2+}, as compared to the corresponding SCF second-order supermolecule terms. As a first step in such an evaluation, we have investigated a series of oligohydrated complexes of Zn^{2+} and a mixed Zn^{2+}–formate–water complex.

With Zn^{2+} along the external bisectors of the bound water molecules (except in 2d below), the investigated complexes are as follows:

1. Zn^{2+} $(H_2O)_2$ for distances, d, ranging from 1.8 to 2.2 Å. Two distinct configurations are compared, with the θ angle (Ow_a—Zn—Ow_b) set at either 180° or 90°. A third distinct configuration will be investigated, so that Zn^{2+} is directly bound to solely one water (W_a) at the fixed distance 1.9 Å, and the second water, W_b, is H bonded to W_a at three distinct distances.
2. Zn^{2+} $(H_2O)_4$. Four distinct configurations are compared: (a) square planar; (b) as in 2a, but with one water molecule removed from the plane and lying along the perpendicular to the plane passing through Zn^{2+}; (c) tetrahedral; (d) energy-minimized tetrahedral with the water H's rotated toward the neighboring

water oxygens (D. R. Garmer, private communication).

3. Zn^{2+} $(H_2O)_6$ in an octahedral arrangement. Zn^{2+} is the center of the octahedron, and the Zn—O distances are set at 2.1 Å, corresponding to the best distance found in 2c.
4. To probe the nonadditive behavior of both the E_{pol} and E_{ct} second terms when Zn^{2+} is bound to an anionic ligand, we have investigated a mixed complex in which Zn^{2+} is coordinated simultaneously to formate and water. In the configuration we have selected, formate is fixed in the bidentate configuration and water is maintained in the trans (180°) position. Five different combinations of Zn—C and Zn—Ow_a distances were compared.

A separate evaluation of the nonadditivity of E_1(SCF) showed this quantity to be considerably smaller than that of E_2(SCF) (unpublished data, available upon request). We therefore concentrate here only on the latter terms.

In Tables VIIIA–D, two methods of computing E_{pol} are provided. In the first, (a), the polarizing field on each polarizable center, P, of each individual molecule is computed with the sole permanent monopoles of the cation and all the other molecules. In the second, (b), it is computed with the complete multipolar expansion, including the effect of the induced dipoles, following a standard iterative procedure (see, e.g., refs. 55 and 65 and refs. therein). Denoted by E^0 and E, respectively, the complete fields due to the permanent multipoles and permanent multipoles + induced dipoles, the expression of $E_{pol}(P)$ is then

$$E_{pol}(P) = -0.5 \sum_i E_P^0(i) \sum_j \alpha_P(i,j) E_P(j)$$

The values of E_2 reported in Tables VIII use procedure (a).

Zn^{2+} $(H_2O)_2$

Table VIIIA shows that ΔE(SCF) is significantly larger, at a given Zn—O distance, for $\theta = 180°$ than for $\theta = 90°$, on account of the larger interligand separations occurring with the larger θ. E_1 and, within E_2, E_{pol} contribute with comparable weights to the overall energy difference. The smaller values of E_{pol} for $\theta = 90°$ are themselves due to the increased ligand–ligand interactions, which tend to reduce the net polarizing electric

TABLE VIIIA.
Dihydrated Complexes of Zn^{2+}.

	Arrangement a				
dZn—O =	1.8	1.9	2.0	2.1	2.2
	SCF Results				
ΔE	−151.8	−159.7	−159.8	−155.0	−147.6
E_1	−59.8	−76.0	−83.5	−85.6	−84.4
E_{pol}	−70.3	−65.9	−61.3	−56.3	−51.2
E_{ct}	−21.7	−17.8	−14.9	−13.1	−12.0
E_2	−92.0	−83.7	−76.2	−69.4	−63.2
	SMM Results				
ΔE	−147.2	−157.9	−158.9	−154.1	−146.3
E_1	−59.7	−75.9	−83.2	−85.1	−83.9
$E_{pol}{}_a$	−70.7	−66.8	−62.3	−57.4	−52.4
E_{pol}	−70.5	−66.4	−61.8	−56.9	−52.0
E_{ct}	−16.8	−15.2	−13.4	−11.7	−10.0
E_2	−87.5	−82.0	−73.7	−69.1	−62.4
	Arrangement b				
dZn—O =	1.8	1.9	2.0	2.1	
	SCF Results				
ΔE	−130.2	−143.0	−146.4	−144.4	
E_1	−48.5	−68.4	−78.1	−81.8	
E_{pol}	−63.8	−59.7	−56.0	−51.4	
E_{ct}	−17.9	−15.0	−12.6	−11.2	
E_2	−81.7	−74.7	−68.6	−62.6	
	SMM Results				
ΔE	−134.1	−147.9	−150.9	−147.6	
E_1	−51.4	−70.2	−79.1	−82.0	
$E_{pol}{}_a$	−64.7	−61.5	−57.6	−53.4	
E_{pol}	−63.0	−59.8	−56.0	−51.9	
E_{ct}	−18.0	−16.1	−14.1	−12.2	
E_2	−82.7	−77.6	−71.7	−65.6	
	Arrangement c				
$d$$Ow_a$—$Ow_b$ =	2.85	2.95	3.05		
	SCF Results				
ΔE	−111.3	−110.1	−108.8		
E_1	−53.5	−53.8	−53.8		
E_2	−57.8	−56.2	−55.0		
	SMM Results				
ΔE	−113.4	−112.5	−111.2		
E_1	−52.9	−53.5	−53.6		
$E_{pol}{}_a$	−46.5	−45.4	−44.4		
E_{pol}	−48.7	−47.2	−46.0		
E_{ct}	−14.1	−13.6	−13.2		
E_2	−60.6	−59.0	−57.6		

[a]Value computed with the full multipolar field, including the contribution from the induced dipoles.
Three different arrangements are compared: (a) Zn^{2+} interposed between W_a and W_b, and the angle θ = Ow_a—Zn—Ow_b = 180; (b) θ = 90; (c) W_b is in an outer hydration shell of Zn^{2+} and is H bonded to W_a.
Energies in kcal/mol, distances in Å.

TABLE VIIIB.
Oligohydrates of Zn^{2+}.

Tetra-hydrates	$Zn^{2+}(H_2O)_4$ (a)	(b)	(c)	(d)	Hexa-hydrate
dZn—O	2.1	2.1	2.1	2.0	2.1
	SCF Results				
ΔE	−246.0	−243.4	−233.6	−260.0	−303.6
E_1	−153.1	−152.9	−138.5	−155.9	−204.8
E_{pol}	−78.6	−76.2	−80.6	−88.2	−83.9
E_{ct}	−14.4	−14.3	−14.4	−15.9	−14.9
E_2	−93.0	−90.5	−95.0	−104.1	−98.8
	SMM Results				
ΔE	−251.2	−246.4	−240.2	−262.1	−310.4
E_1	−152.7	−152.1	−142.1	−156.4	−210.6
E_{pol}	−84.1	−80.2	−83.6	−91.9	−86.1
E_{pol}*	−79.1	−76.0	−79.5	−87.3	−82.2
E_{ct}	−14.4	−14.1	−14.5	−14.8	−13.7
E_2	−98.5	−94.3	−98.1	−105.7	−99.8

Note: Energies in kcal/mol, distances in Å. (a) Square planar; (b) one water apical; (c) pyramidal; (d) pyramidal, energy minimized.
* Value computed with the full multipolar field, including the contribution from the induced dipoles.

TABLE VIIIC.
Binding Energetics in a Mixed Formate–Zn^{2+}–Water Complex.

dZn—Ow =	1.9	2.0	2.1	2.0	2.1
dZn—C =	2.2	2.2	2.2	2.3	2.3
	SCF Results				
ΔE	−427.0	−428.7	−428.0	−429.4	−428.6
E_1	−316.1	−320.3	−321.6	−325.0	−326.4
E_{pol}	−86.6	−84.9	−83.2	−82.1	−80.3
E_{ct}	−24.3	−23.9	−23.2	−22.3	−22.0
E_2	−110.9	−108.8	−106.4	−104.4	−102.3
	SMM Results				
ΔE	−428.0	−429.7	−430.3	−432.9	−432.5
E_1	−315.0	−318.9	−320.3	−326.1	−327.4
E_{pol}	−90.2	−88.7	−87.2	−84.8	−83.1
E_{pol}[a]	−88.9	−87.6	−86.3	−83.5	−82.0
E_{ct}	−22.8	−22.8	−23.0	−22.0	−22.1
E_2	−113.0	−111.5	−109.2	−106.8	−105.2

Zn^{2+} bridges the two anionic oxygens and lies along the external bisector of water. Energies in kcal/mol, distances in Å.
[a] Value computed with the full multipolar field, including the contribution from the induced dipoles.

field felt by any one ligand. E_{ct}(SCF) itself displays a larger preference for $\theta = 180°$ over $\theta = 90°$, but it is less pronounced than those of E_1 and E_{pol}. Such trends of ΔE(SCF), E_1, and E_{pol} are closely reproduced by the corresponding SMM terms, and the numerical match is close. On the other hand, E_{ct}(SMM) is virtually insensitive, at a given Zn—O distance, to either value of θ, but because it has values which are intermediate between the SCF ones for the two values of θ, the numerical agreement between E_{ct}(SMM) and E_{ct}(SCF) remains satisfactory.

Upon studying the outer-shell binding of Zn^{2+} to one water molecule, W_b, we did not perform a decomposition of E_2(SCF) into E_{pol} and E_{ct}, because this would require a further breakdown of E_{ct} into the charge transfer from W_a to Zn^{2+}, as well as that from W_b to W_a, and we thus report E_2(SCF) alone. ΔE(SMM) matches ΔE(SCF) to within 2 kcal/mol out of 110, while E_1(SMM) matches E_1(SCF) to within 0.5 kcal/mol. Computation of E_{pol} according to (b) provides a better numerical agreement with E_{pol}(SCF) than (a) in the first two configurations, but a less satisfactory one in the outer-shell configurations.

$Zn^{2+}(H_2O)_4$

The results are reported in Table VIIIB for the best dZn—O distances in the four investigated arrangements. The SCF energy ordering of the four arrangements, $d > a > b > c$, is correctly reproduced by the SMM procedure, with the values of ΔE(SMM) matching the corresponding SCF ones to within 7 kcal/mol out of approximately 250. It is noteworthy that the 14 kcal/mol SCF preference for d over a stems predominantly from the E_2 term accounting for 11.1 kcal/mol (with E_{pol} accounting for 9.6 kcal/mol), whereas E_1 contributes solely 2.8 kcal/mol to this preference. The greater importance of the E_2 over the E_1 difference is accounted for in the corresponding SMM computations (8.2 versus 3.7 kcal/mol within a total energy difference of 12 kcal/mol).

The nonadditive behaviors of E_{pol} and E_{ct} can be exemplified by comparing the increase in their numerical values upon passing from the monohydrate (d = 2.1 Å) to the representative square planar tetrahydrate a. Thus, E_{pol}(SCF) and E_{ct}(SCF) increase respectively by factors of 2.5 and 1.9 when the number of ligands is multiplied by 4. Correspondingly, E_{pol}(SMM) and E_{ct}(SMM) increase, respectively, by factors of 2.8 and 1.9: At this level of treatment, this should lend confidence in the stability of our SMM formulation of these two terms as a function of increasing the Zn^{2+} coordination. The numerical match of E_{pol}(SMM) to its SCF counterpart is somewhat downgraded with respect to the $Zn^{2+}(H_2O)_2$ complexes. This is the most pronounced in complex a, where E_{pol}(SMM) is

overestimated with respect to E_{pol}(SCF) by 5.5 kcal/mol out of 79 (i.e., 7%). Computation of E_{pol}(SMM) according to (b) improves the agreement.

Zn^{2+} $(H_2O)_6$

Zn^{2+} with a complete first-solvation shell model provides a crucial test for the robustness of the present formulation of E_{pol} and E_{ct}, and their nonadditive behaviors, within the SMM procedure. It is observed that E_1(SMM) matches E_1(SCF) to within 6 kcal/mol out of 206, and that E_2(SMM) matches its SCF counterpart to within 1 kcal/mol out of 100. ΔE(SMM) is able to match ΔE(SCF) to within 7 kcal/mol out of 305.

The nonadditive behaviors of E_{pol} and E_{ct} can be again exemplified if we compare the evolution of their numerical values upon passing from the Zn^{2+}–H_2O complex at a Zn—O distance of 2.1 Å, to the $Zn^{2+}(H_2O)_6$ one. Thus E_{pol}(SCF) is multiplied by a factor of 2.7, and E_{ct}(SCF) is multiplied by a factor of 1.9, whereas the number of ligands is multiplied by 6. The corresponding factors in the SMM procedure are extremely close—namely, 2.8 and 1.9, respectively. The nonadditive behavior of E_{ct} can have some serious implications in attempts to model it, in divalent cation complexes, by simple overlap-dependent terms. A strictly additive approach would result in a value of E_{ct} amounting to 45.6 kcal/mol in this hexaligand complex, introducing thus a numerical error of 31 kcal/mol.

Formate–Zn^{2+}–Water

The results are reported in Table VIIC. It is instructive to compare them to those found with the corresponding in-plane unhydrated bidentate Zn^{2+} complex. ΔE(SMM) matches ΔE(SCF) to within 4 kcal/mol out of 430 (i.e., to within 1%), an agreement that is even better than in the unhydrated complex. It is noteworthy that E_{ct}(SCF) actually decreases (by 1.0 kcal/mol at dZn—O = 2.2 Å) upon passing from the unhydrated to the monohydrated complex, and this trend is also shown by E_{ct}(SMM), although it is somewhat amplified here, with a corresponding decrease of 2.6 kcal/mol. More extensive comparisons between the SCF and SMM second-order values, bearing on several other binding configurations and other ligands, are clearly needed to ascertain the quality of the present formulation. The present results are nevertheless extremely encouraging.

Although in Tables VIIIA–C procedure (b) improves the fit to E_{pol}(SCF) with respect to procedure (a), it is more computationally demanding. It has also provided a less satisfactory agreement in the case of outer-shell binding of water to Zn^{2+}. These facts, together with the satisfactory results obtained with (a) throughout the present tests, should justify the use of (a) in future large-scale simulations.

Conclusions

The present investigation focuses primarily on the monoligated complexes of Zn^{2+} with water, the end sidechains of His, Asn, Gln, Cys, as well as with the anionic ligands formate, hydroxy, and methanethiolate. These constitute the most commonly encountered Zn^{2+}-binding ligands within the active sites of metalloenzymes. Our purpose is to probe the ability of the SMM procedure to reproduce, with a minimal number of nontransferable parameters, the results of our previously reported *ab initio* SCF supermolecular computations on these complexes.[17] Important refinements to the SMM procedure, prompted by the availability of these results are as follows:

—The computation of the electrostatic term E_{MTP} with the help of distributed multipoles derived from high-quality Gaussian basis functions

—An anisotropic formulation of the short-range repulsion energy E_{rep}

—The computation of E_{pol} with the help of distributed anisotropic polarizabilities and with a Gaussian screening of the electrostatic field

—The introduction, within the expression of E_{ct}, of a coupling with the polarization.

The evolutions of each separate energy term in the SMM procedure—E_{MTP}, E_{rep}, E_{pol}, and E_{ct}—are scrutinized by performing radial as well as in- and out-of-plane angular variations of the position of Zn^{2+}, and systematic comparisons were undertaken with the reported[17] behaviors of the corresponding *ab initio* supermolecular energy terms using the RVS analysis.[22] In agreement with these *ab initio* SCF investigations, the SMM computations have highlighted the following energetical and structural features:

—The important numerical weight of the second-order terms within ΔE. Thus E_2 amounts

to more than half of the total ΔE in the Zn^{2+}–neutral ligand complexes. In the specific Zn^{2+}–methanethiol complex, E_2 amounts to more than 80% of it. In the ionic Zn^{2+}–methanethiolate complex, E_2 still accounts for one third of it.

—The marked nonlinearity in the geometry of the in-plane complexes of Zn^{2+}. Thus, in this cation's complexes with the carbonyl bond, methoxy, methanethiolate, and hydroxy, the best values of θ were found to be 150°, 120°, 105°, and 120°, respectively, rather than 180°. Accounting for such angular preferences with the help of genuine atom-centered molecular mechanics may not be achieved. The present analysis shows such preferences to stem from the electrostatic and charge transfer terms, whereas short-range repulsion and polarization are best at 180°.

—The marked non-coplanarity of Zn^{2+} with respect to the CSH plane in its methanethiol complex as contrasted to its coplanarity with respect to the imidazole and formamide planes in the corresponding complexes, again due to E_{MTP} and E_{ct}.

Each of the SMM energy terms was shown to reproduce faithfully the behavior of the corresponding SCF term upon varying the R, θ, or ϕ geometrical variables, enabling in several cases a numerical match between ΔE(SCF) and ΔE(SMM) to within $< 2\%$. Even though E_{rep} and E_{ct} had similar angular dependencies, their radial dependencies were markedly different, with E_{ct} decreasing in a much slower way than E_{rep}. Conspicuous examples were provided by the Zn^{2+} complexes with methanethiolate and hydroxy. Such a fact, in addition to the strong nonadditive character of E_{ct} (which was evidenced in refs. 17 and 18), indicates that it may be illusory to try and lump together these two short-range components in a single exponential-like expression. On the other hand, we believe that, as far as an accurate reproduction of the SCF RVS supermolecule computations with Zn^{2+} frozen is concerned (and notwithstanding the latters' own limitations—absence of correlation effects, incompleteness of the basis set), the principal default still lingering in the SMM procedure resides in its E_{pol} term. We have observed that E_{pol}(SMM) is systematically underestimated with respect to E_{pol}(SCF) in the complexes of Zn^{2+} with oxygen ligands (but not with sulfur ligands) whenever θ is close to 120° (i.e., when the cation lies along the direction of one O lone pair) and that such an underestimation tends to increase upon increasing the cation—O distance by up to 0.3 Å from equilibrium distance. In the complexes of Zn^{2+} with carbonyl and carboxylate ligands, it was not possible to account for the shallow behavior (and actual increase) which occurs upon rotating Zn^{2+} on a cone having the C—O bond as an axis, as the cation moves toward the perpendicular to the HCO plane: This rotation leads to a small but pronounced decrease of E_{pol}(SMM), consistent with the smaller out-of-plane than in-plane values of the polarizability tensor on the carbonyl. This is indicative of higher order effects within E_{pol}(SCF) not accounted for in the expression of E_{pol}(SMM), which is limited to dipole polarizabilities. The incidence of such effects may be limited, however, in polyligated complexes of Zn^{2+}, where, as observed in ref. 17, the reduction of the Zn^{2+} polarizing field on a given ligand due to all the other ones is likely to affect them more than the dipole polarizability effects.

A reliable handling of the nonadditivity effects occurring in polyligated complexes of Zn^{2+} is mandatory for prospective application of the SMM procedure to Zn^{2+}–oligopeptide, Zn^{2+}–ionophore, and Zn^{2+}–enzyme inhibitor complexes. In all oligoligated complexes reported here, the nonadditive behaviors of both E_{pol}(SCF) and E_{ct}(SCF) could be closely accounted for by their SMM counterparts, without the need to resort to extraneous three-body terms.

We have recently reported[28] the results of a joint *ab initio* SCF/density functional theory/SMM study devoted to a series of hydrogen-bonded complexes involving uncharged as well as charged entities. The encouraging results, in conjunction with the present ones, have prompted an application of the SMM procedure to studies of complexes formed between the active site of a metalloenzyme, thermolysin, and a series of inhibitors. These will be reported in a forthcoming article. An updated version of the SIBFA program (present QCPE release under number 614) should be released in the near future.

Acknowledgments

The computations reported in this article were done during a sabbatical stay at the Center for Advanced Research in Biotechnology. The author wishes to express his sincere gratitude and appreciation to Walter J. Stevens and Morris Krauss for numerous and illuminating discussions during the

course of this work. These have exerted a decisive influence on the refinement of the SMM procedure.

Tables IA, IB, IIIB, IV, VIA, and VIIB (marked with an asterisk in the text) are available as supplementary material from the author.

Appendix

Values of the Parameters Used in the Calibration of the SMM Procedure.

1. Effective radii (angstrom)

Atom Ligand	H	C	*N*-pyridine Imidazole	*O*-hydroxyl Water	*O*-carbonyl Formamide	*S*-(thiol) Methanethiol
W	1.70	1.70	1.70	1.50	1.50	1.925
V	1.20	1.70	1.60	1.50	1.425	1.60
U		1.00	1.65	1.50	1.45	1.65

Atom Ligand	*O*-carboxylate Formate	*O*-(alkoxy) Methoxy	*O*-(hydroxy) Hydroxy	*S*-(thiolate) Methanethiolate
W	1.50	1.625	1.90	2.40
V	1.625	1.55	1.625	1.80
U	1.85	1.70	1.625	2.35

2. Screening factors E and F

Ligand	Imidazole	Water	Formamide	Methanethiol
E	0.66[a] 0.90[b]	0.68	0.68	0.68
F	1.95[a] 1.40[b]	1.40	1.40	1.54

Ligand	Formate	Methoxy	Hydroxy	Methanethiolate
E	0.80	0.78	0.68	0.68
F	1.45	1.60	1.40	1.65

3. Zn parameters used in the expression of E_{rep}

W_{Zn}	K(Zn—H)	K(Zn—C)	K(Zn—N)	K(Zn—O)	K(Zn—S)	m_{PM}
1.235	15.68	15.68	17.38	18.81	12.0	1.0[c] 1.87[d]

4. Parameters used in the expression of E_{ct}

I	J	η	$S_M(Zn^{2+})$	$D_M(Zn^{2+})$	t_{AsM}	t_{ApM}
3.75	0.75	9.5	2.71	2.50	0.39[e] 0.33[f] 0.33[g]	0.57[e] 0.51[f] 0.54[g]
					m_{AM} 0.57[e] 0.52[f] 0.90[g]	

These values are given for energies expressed in Kcal / mol, and distances and effective radii expressed in angstrom units (Å).

[a] Lone pair polarizabilities.

[b] Bond polarizabilities.

[c] P = oxygen or nitrogen ligand.

[d] P = sulfur ligand.

[e] A = nitrogen atom.

[f] A = oxygen atom.

[g] A = sulfur atom.

References

1. B. W. Matthews, *Acc. Chem. Res.*, **21,** 333 (1988).
2. H. Kim and W. N. Lipscomb, *Biochemistry*, **29,** 5546 (1990).
3. D. N. Silverman and S. Lindskog, *Acc. Chem. Res.*, **21,** 30 (1988).
4. B. P. Roques, F. Noble, V. Daugé, M.-C. Fournié-Zaluski, and A. Beaumont, *Pharmacol. Rev.*, **45,** 88 (1993).
5. M. A. Ondetti and D. W. Cushman, *Crit. Rev. Biochem.*, **16,** 381 (1984).
6. D. W. Christianson and W. N. Lipscomb, *Accounts Chem. Res.*, **22,** 62 (1989).
7. W. Bode, F.-X. Gomis-Ruth, and W. Stockler, *FEBS Lett.*, **331,** 134 (1993).
8. J. M. Berg, *Science*, **232,** 485 (1986).
9. D. Demoulin and A. Pullman, *Theoret. Chim. Acta*, **49,** 161 (1978).
10. V. Kothekar, A. Pullman, and D. Demoulin, *Int. J. Quant. Chem.*, **14,** 779 (1978).
11. O. Jacob, R. Cardenas, and O. Tapia, *J. Am. Chem. Soc.*, **112,** 8692 (1990).
12. A. Alex and T. Clark, *J. Comp. Chem.*, **13,** 704 (1992).
13. M. Krauss and D. R. Garmer, *J. Am. Chem. Soc.*, **113,** 6426 (1991).
14. K. M. Merz, Jr., R. Hoffman, and M. J. S. Dewar, *J. Am. Chem. Soc.*, **111,** 5636 (1989).
15. C. Giessner-Prettre and O. Jacob, *J. Comp.-Aided Mol. Design*, **3,** 23 (1989).
16. K. M. Merz and P. A. Kollman, *J. Am. Chem. Soc.*, **111,** 6426 (1989).
17. N. Gresh, W. J. Stevens, and M. Krauss, *J. Comp. Chem.*, **16,** 843 (1995).
18. D. R. Garmer and N. Gresh, *J. Am. Chem. Soc.*, **116,** 3556 (1994).
19. M. A. Holmes and B. W. Matthews, *Biochemistry*, **20,** 6912 (1981).
20. A. R. Fersht, *Enzyme Structure and Mechanism*, W. H. Freeman, New York, 1985.
21. B. P. Roques, M.-C. Fournié-Zaluski, E. Soroca, J. M. Lecomte, B. Malfroy, C. Llorens, and J. C. Schwartz, *Nature*, **288,** 286 (1980).
22. W. J. Stevens and W. Fink, *Chem. Phys. Lett.*, **139,** 15 (1987).
23. N. Gresh, P. Claverie, and A. Pullman, *Theoret. Chim. Acta*, **20,** 1 (1984).
24. N. Gresh, P. Claverie, and A. Pullman, *Int. J. Quantum Chem.*, **29,** 101 (1986).
25. N. Gresh, P. Claverie, and A. Pullman, *Int. J. Quantum Chem.*, **28,** 757 (1985).
26. K. Kitaura and K. Morokuma, *Int. J. Quantum Chem.*, **10,** 325 (1976).
27. R. Cammi, H.-J. Hofmann, and J. Tomasi, *Theoret. Chim. Acta*, **76,** 297 (1989).
28. N. Gresh, M. Leboeuf, and D. R. Salahub, in: Modeling the Hydrogen Bond, A.C.S. Symposium series 569, D. A. Smith, Ed., 82 (1994).
29. W. J. Stevens, H. Basch, and M. Krauss, *J. Chem. Phys.*, **81,** 6026 (1984).
30. S. Creuzet, J. Langlet, and N. Gresh, *J. Chim. Phys.*, **88,** 2399 (1991).
31. F. Vigné-Maeder and P. Claverie, *J. Chem. Phys.*, **88,** 4988 (1988).
32. J. A. C. Rullmann and P. Th. van Duijnen, *Reports Mol. Theory*, **1,** 1 (1990), and refs. therein.
33. S. L. Price and A. J. Stone, *Mol. Phys.*, **47,** 1457 (1982).
34. R. Wheatley and S. L. Price, *Mol. Phys.*, **69,** 507 (1990).
35. A. J. Stone and S. L. Price, *J. Phys. Chem.*, **92,** 3325 (1988).
36. S. L. Price and A. J. Stone, *Mol. Phys.*, **51,** 569 (1984).
37. J. Mitchell and S. L. Price, *J. Comp. Chem.*, **11,** 1217 (1990).
38. J. N. Murrell and J. J. C. Teixeira-Dias, *Mol. Phys.*, **19,** 521 (1970).
39. P. Claverie, In *Intermolecular Interactions, from Diatomics to Biopolymers*, B. Pullman, Ed., John Wiley & Sons, New York, 1978, p. 69.
40. Y. S. Kim, S. K. Kim, and W. Don Lee, *Chem. Phys. Lett.*, **80,** 574 (1981).
41. A. J. Stone, *Mol. Phys.*, **56,** 1065 (1985).
42. D. R. Garmer and W. J. Stevens, *J. Phys. Chem.*, **93,** 8263 (1989).
43. (a) M. Dupuis and H. F. King, *Int. J. Quantum Chem.*, **11,** 613 (1977); (b) M. Dupuis and H. F. King, *J. Chem. Phys.*, **68,** 3998 (1978).
44. N. Gresh, P. Claverie, and A. Pullman, *Int. J. Quantum Chem.*, **Symp. 13,** 243 (1979).
45. J. Langlet, P. Claverie, F. Caron, and J.-C. Boeuve, *Int. J. Quantum Chem.*, **20,** 299 (1981).
46. J. N. Murrell, M. Randic, and D. R. Williams, *Proc. Roy. Soc. London*, Ser. A, **284,** 566 (1966).
47. N. Gresh, P. Claverie, and A. Pullman, *Int. J. Quantum Chem.*, **22,** 199 (1982).
48. E. Clementi and D. Raimondi, *J. Chem. Phys.*, **38,** 2686 (1963).
49. C. E. Moore, *Atomic Energy Levels*, National Bureau of Standards, Circ. 467, U.S. Government Printing Office, Washington, DC, 1949.
50. W. Meyer, *Int. J. Quantum Chem.*, **5,** 341 (1971).
51. A. Baker, C. Baker, C. Brundle, and D. Turner, *Int. J. Mass Spectrom. Ion Phys.*, **1,** 285 (1968).
52. H. Berthod and A. Pullman, *J. Comp. Chem.*, **2,** 87 (1981).
53. B. Pullman, N. Gresh, H. Berthod, and A. Pullman, *Theoret. Chim. Acta*, **44,** 151 (1977).
54. A. J. Stone and M. Alderton, *Mol. Phys.*, **56,** 1047 (1985).
55. T. P. Lybrand and P. A. Kollman, *J. Chem. Phys.*, **83,** 2923 (1985).
56. J. W. Caldwell and P. A. Kollman, *J. Phys. Chem.*, **96,** 8249 (1992).
57. L. X. Dang, *J. Chem. Phys.*, **96,** 6970 (1992).
58. O. A. Karim, *Chem. Phys. Lett.*, **184,** 560 (1991).
59. M. Sprik, *J. Phys. Chem.*, **95,** 2283 (1991).
60. S. Roderick, M.-C. Fournié-Zaluski, B. P. Roques, and B. W. Matthews, *Biochemistry*, **28,** 1493 (1989).
61. I. Ortega-Blake, O. Novaro, A. Les, and S. Rybak, *J. Chem. Phys.*, **76,** 5405 (1982).
62. L. A. Curtiss, J. W. Halley, and J. Hautman, *Chem. Phys. Lett.*, **133,** 89 (1989).
63. E. Kochanski, *Chem. Phys. Lett.*, **133,** 143 (1987).
64. J. Caldwell, I. Dang, and P. A. Kollman, *J. Am. Chem. Soc.*, **112,** 9144 (1990).
65. A. J. Stone, *Chem. Phys. Lett.*, **155,** 111 (1989).